RSC Medicinal Chemistry

Accepted Manuscript

This article can be cited before page numbers have been issued, to do this please use: R. Choudhary, V. Duvauchelle, C. Lindgren, K. Stangner, S. Knutsson, N. Forsgren, F. Ekström, L. Kamau and A. Linusson Jonsson, *RSC Med. Chem.*, 2025, DOI: 10.1039/D5MD00797F.

ROYAL SOCIETY OF CHEMISTRY

rsc.li/medchem

View Article Online
DOI: 10.1039/D5MD00797F

Potent and Selective Indole-based Inhibitors Targeting Disease-Transmitting Mosquitoes

R. Rajeshwari[1], V. Duvauchelle[1], C. Lindgren[1], K. Stangner[1], S. Knutsson[1], N. Forsgren[2], F. Ekström[2], L. Kamau[3], A. Linusson*[1]

[1]*Department of Chemistry, Umeå University (Sweden);* [2]*Swedish Defense Research Agency, Umeå (Sweden);* [3]*Centre of Biotechnology Research and Development, Kenya Medical Research Institute, Nairobi, Kenya*
*Corresponding author. E-mail address: anna.linusson@umu.se

Abstract
Vector control with insecticides is an important preventive measure against mosquito borne-infectious diseases, such as malaria and dengue. The intensive usage of few insecticides has resulted in emerging resistance in mosquitoes, and unwanted off-target toxic effects. Therefore, there is a great interest in alternative active ingredients. Here, we explore indole-based compounds as selective inhibitors against acetylcholinesterase 1 (AChE1) from the disease-transmitting mosquitoes *Anopheles gambiae* (*An. gambiae*, *Ag*AChE1) and *Aedes aegypti* (*Ae. aegypti*, *Ae*AChE1) as potential future candidates as insecticides for vector control. Three sets of compounds were designed to explore their structure-activity relationship, and investigate their potentials regarding potency and selectivity. 26 indole-based compounds were synthesised and biochemically evaluated for inhibition against *Ag*AChE1, *Ae*AChE1 and human AChE (*h*AChE). The compounds showed to be potent inhibitors against AChE1, and selective for AChE1 over *h*AChE. N-Methylation of the indole moiety clearly increased the inhibition activity, and a bulkier benzyl moiety improved the selectivity. X-ray crystallography shows that the inhibitors bind in the bottom of the active site gorge of mouse AChE (*m*AChE), while molecular dynamics simulations revealed different binding poses in *m*AChE and *Ag*AChE1. Four potent and selective inhibitors were subjected to in vivo mosquito testing. Topical application showed strong insecticidal effects on *An. gambiae* and *Ae. aegypti*, highlighting this compound class as an interesting alternative for future insecticide research.

Introduction

Anopheles gambiae (An. gambiae), and *Aedes aegypti* (*Ae. aegypti*) are disease-transmitting mosquitoes, so called vectors, that spread diseases such as malaria, dengue, chikungunya, yellow fever and Zika. Vector control by the use of insecticides is an important preventive measure against mosquito-borne infectious diseases, including malaria. The insecticides used in vector control belong mainly to four chemical classes, organophosphates, carbamates, hydrocarbons, and pyrethroids. In malaria-endemic countries consistent implementation of insecticide-treated mosquito nets with pyrethroids have resulted in significant public health impact.[1-3] Unfortunately, the widespread usage of insecticides has also led to the development and spread of insecticide-resistant mosquito populations, for example, metabolic detoxification in mosquitoes and target site structural mutations,[4, 5] resulting in a need for new insecticides.

View Article Online
DOI: 10.1039/D5MD00797F

Acetylcholinesterase (AChE) is the insecticidal target of organophosphates and carbamates, while hydrocarbons and pyrethroids target voltage-gated channels; both targets are present in the mosquitoes' nervous system. The insecticidal activity of organophosphates and carbamates is achieved through covalent modification (phosphorylating or carbamoylating) of the conserved catalytic serine residue at the bottom of a deep active site gorge of AChE (Figure 1). The active sites of AChEs of different organisms are highly conserved. Hence, the currently used organophosphates and carbamates are nonspecific and inhibits AChEs from different organisms, including human (*h*AChE),[6, 7] leading to off-target toxicity.[8] AChE is an essential enzyme that terminates cholinergic nerve signaling by hydrolyzing the neurotransmitter acetylcholine (ACh).[9] Inhibition of AChE leads to continuous nerve signaling due to accumulation of ACh in the synaptic cleft, and eventually to paralysis and death of the organism. The active site gorge is lined with aromatic amino acid residues, and consists of a peripheral site (PS) at the entrance of the gorge and the catalytic site (CAS) at the bottom (Figure 1).[10] In mosquitoes and many other insects, AChE is encoded by two genes called *ace-1* and *ace-2*,[11, 12] in contrast to vertebrates that only have one gene. The *ace-1* encoded AChE1 is the main catalytically active enzyme in mosquito.[12]

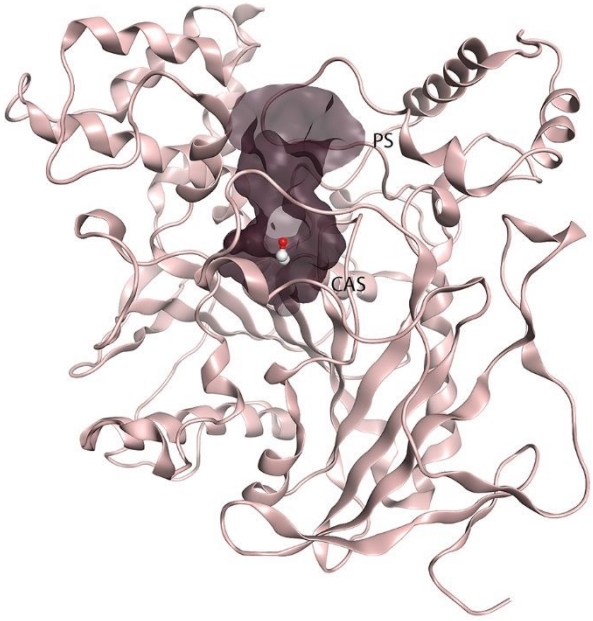

Figure 1. The 3D structure of AChE1 of *An. gambiae* (*Ag*AChE1), with the active site gorge displayed in grey and the conserved catalytic serine highlighted in ball and sticks (PDB: 5X61). The peripheral- (PS) and catalytic sites (CAS) are shown.

*Ag*AChE1 and mammalian AChEs, such as *h*AChE and mouse (*m*AChE), share highly similar overall structures, including the conserved catalytic triad in the active site gorge. However, notable differences exist in the loops that line the entrance to the active site gorge.[13] These loops vary in length, conformation, and residue composition between mosquito and mammalian AChEs, creating differences in the shape and accessibility of the gorge. These variations may influence ligand binding and offer opportunities for the design of selective inhibitors. To meet the need for new insecticides while minimizing off-target toxicity, selective inhibition of mosquito AChE1 over hAChE using noncovalent inhibitors has emerged as an

View Article Online
DOI: 10.1039/D5MD00797F

attractive strategy.[14] In recent years, significant efforts have been made to discover potent noncovalent mosquito AChE1 inhibitors with in vivo insecticidal activity.[15-18] Here, we have designed and synthesized indole-based compounds to target AChE1 from *An. gambiae* and *Ae. aegypti* (*Ag*AChE1 and *Aa*AChE1). The synthesized compounds were evaluated in vitro through activity-based assay to investigate potency and selectivity. The interaction patterns of the indole-based inhibitors in complex with *m*AChE were explored by X-ray crystallography and molecular dynamics (MD) simulations. Finally, a few inhibitors were subjected to in vivo testing to establish their insecticidal activity against the mosquito species *An. gambiae* and *Ae. aegypti*.

Results and discussion

Identification of indoles as biologically active scaffold and inhibitor against AChE1

In a previously reported HTS campaign against recombinant AChE1 performed in our laboratory,[14] the indole-based compounds **8**, **10**, and **15** were identified as hits (Figure 2A). The hit compounds significantly reduced the enzymatic activity of *Aa*AChE1 and *Ag*AChE1 at the tested concentration of 50 µM, while not showing any inhibitory activity against *h*AChE. The indole moiety is known as a versatile heterocyclic fragment in medicinal chemistry and to confer antitubercular,[19, 20] antibacterial,[21, 22], antiviral[23] and anti-cancer activities.[24] Interestingly, indole derivatives have also been reported as potential drug candidates against central nervous system disorders and as AChE inhibitors (Figure 2B).[25, 26] Indole-based compounds have also previously been reported as insecticides, although without any knowledge regarding mechanism of action (Figure 2B).[27, 28] The hit compounds were evaluated in silico and, to some extent, experimentally for toxicity endpoints and lead-likeness, and were considered suitable for further development (Tables S1-S2 and Figure S1).

View Article Online
DOI: 10.1039/D5MD00797F

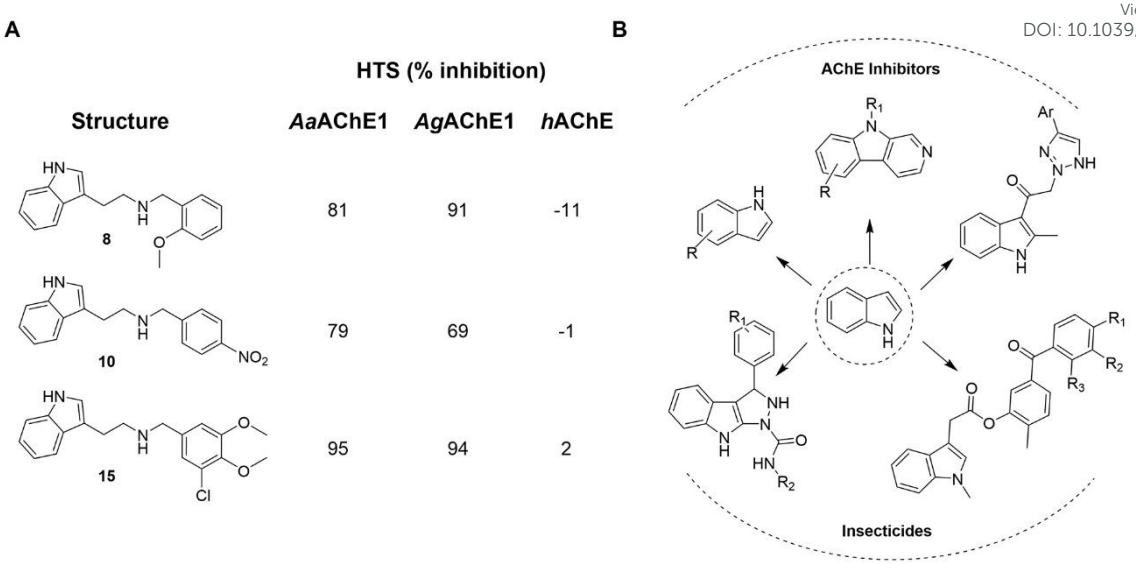

Figure 2. (**A**) Chemical structures and HTS inhibition data of the indole-based hit compounds. (**B**) Previously reported indole-based AChE inhibitors (top),[25, 26] and insecticides (bottom).[27, 29]

Design strategy and synthesis of three sets of indole-based inhibitors

Three sets A-C were designed based on the hit compounds from the HTS (Figure 3). The modifications were chosen to balance electronic and steric effects while maintaining synthetic feasibility. Set A comprised of 12 compounds (**6**-**17**) including the hit compounds **8**, **10**, and **15**, and were designed to investigate the effect of N-methylation (N-Me) of the indole moiety, and the effect of varying the benzyl moiety (Table 1). Set B comprised of nine compounds (**18**-**26**), where the methoxybenzyl moiety was kept constant, and the substituents of the indole (both N-H and N-Me indoles) were varied (Table 2). Set C was designed to investigate changes of the aliphatic linker, through methylations of the secondary amine (**29**-**30**), and the cyclization of the linker chain compounds (**31**-**33)** with the intention of introducing rigidity within the structure (Table 3).

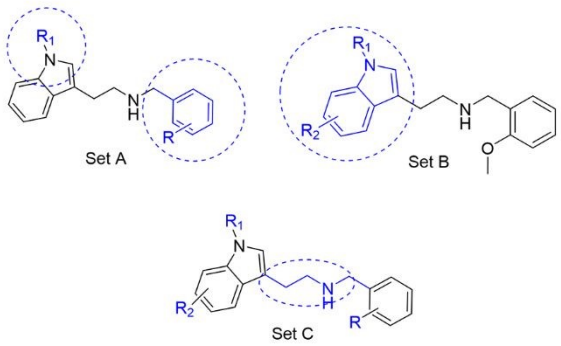

Figure 3. Design strategy of the three sets of molecules (A-C) based on the hit compounds. The explored parts of each set are indicated in blue.

Table 1. Chemical structures and IC_{50} values of N-H and N-methylated indoles in set A.

ID	Structure	*Ag*AChE1 IC_{50} μM[a]	*Aa*AChE1 IC_{50} μM[a]	*h*AChE IC_{50} μM[a]	S.R[b]

View Article Online
DOI: 10.1039/D5MD00797F

6	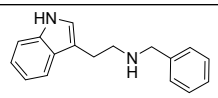	38 (33 - 44)	34 (27 - 41)	> 500	>13
7	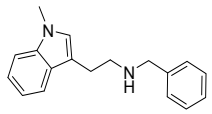	11 (4.1 - 123)	n.d.	115 (94 - 145)	10
8	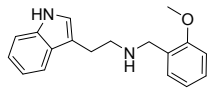	1.6 (1.3 - 2.0)	1.1 (0.9 - 1.4)	70 (39 - 330)	44
9	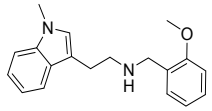	0.06 (0.044 - 0.070)	n.d.	1.6 (1.5–1.7)	27
10	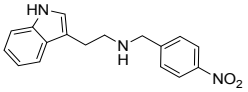	2.2 (1.8 - 2.6)	1.7 (1.4-2.1)	85 (46-321)	39
11	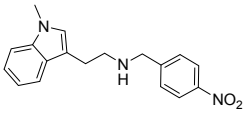	0.2 (0.15 - 0.23)	n.d.	6.6 (5.4-8.0)	33
12	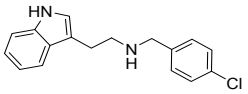	20 (11 - 43)	n.d.	>200	13
13	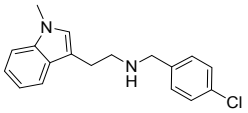	1.5 (1.0 - 2.2)	n.d	74 (60–95)	49
14	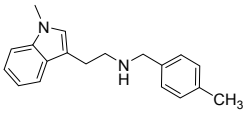	13 (6.3 - 36)	n.d.	124 (98 - 169)	10
15	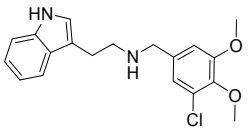	0.72 (0.67 - 0.78)	0.71 (0.62-0.81)	284 (166-903)	394
16	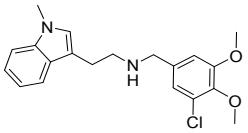	0.04 (0.031 - 0.05)	n.d.	14 (12–16)	350
17	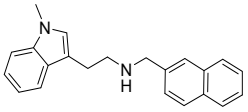	0.51 (0.40 - 0.65)	n.d.	14 (9.6–21)	27

[a]Compounds tested as HCl salts unless specified, values given in parentheses = 95% confidence interval; n.d. refers to not determined; [b]S.R. = selectivity ratios were calculated by taking the compound's IC_{50} for *h*AChE and dividing by its values for *Ag*AChE1.

Table 2. Chemical structures and IC_{50} values of substituted indoles in set B.

ID	Structure	***Ag*AChE1** IC_{50} μM[a]	***h*AChE** IC_{50} μM[a]	**S.R**[b]

View Article Online
DOI: 10.1039/D5MD00797F

18	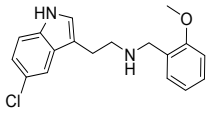	0.4 (0.21 - 0.60)	62 (54 - 71)	155
19	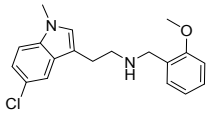	0.07 (0.04 - 0.1)	4.3 (2.7 - 6.7)	61
20	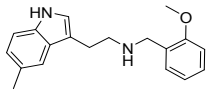	2.7 (2.3 - 3.1)	93 (80 - 111)	34
21	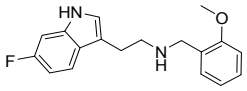	1.6 (1.3 - 2.0)	53 (46 - 61)	33
22	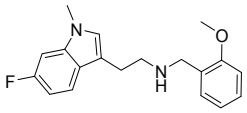	0.2 (0.1 - 2.8)	3.5 (2.9 - 4.2)	17
23	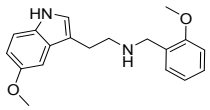	48 (24 - 110)	156 (128 - 216)	3
24	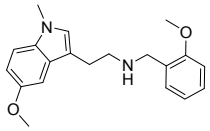	3.2 (1.0 - 11)	18 (13 - 27)	6
25	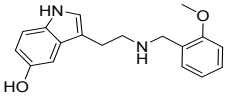	16 (11 - 23)	93 (52-527)	6
26	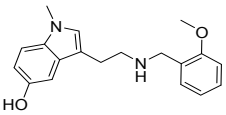	2.1 (1.1 - 3.9)	17 (10 - 34)	8

[a]Compounds tested as HCl salts unless specified, values given in parentheses = 95% confidence interval; [b]S.R = selectivity ratios were calculated by taking the compound's IC_{50} for *h*AChE and dividing by its values for *Ag*AChE1.

The derivatives in sets A and B were synthesized following two different pathways (Scheme 1). On one hand, N-H indole derivatives **6**, **8**, **10**, **12**, **15, 18**, **20**, **21**, **23**, and **25** (Tables 1-2) were reached through a one-pot direct reductive amination between the commercially available tryptamines **1a-f** and benzaldehydes **2a-f** (Figures S2-S3) in ethanol at rt or under reflux condition, and further reduced by $NaBH_4$ or $NaCNBH_3$ to afford N-H indoles analogues in a 32-70% yield after purification over column chromatography (Scheme 1A). On the other hand, analogues **7**, **9**, **11**, **13**, **14**, **16**, **17**, **19**, **22**, **24**, and **26** (Tables 1-2) involved the synthesis of the N-methylated indole derivatives before performing the reductive amination. The chemical route involved the transitory Boc protection of the primary amine of commercially available tryptamines 1a–f, affording intermediates 3a–e in 84–92% yield after purification by column chromatography. The N-methylation was then performed in the presence of NaH and MeI to provide **4a-e** in a 64-85% yield after purification over column chromatography, followed by the Boc-group cleavage in the presence of TFA in DCM to afford **5a-e** intermediates with a 66-85% yield without further purification (Scheme 1B). The intermediate **5f** was synthesized by a different method, as presented in Scheme S1. Further, the one-pot

View Article Online
DOI: 10.1039/D5MD00797F

reductive amination of N-alkylated derivatives **5a-f** with the benzaldehydes **2a-g**, using $NaBH_4$ as a reductive agent was performed and directly followed by the formation of the corresponding ammonium chloride salts **7**, **9**, **11**, **13**, **14**, **16**, **17**, **19**, **22**, **24**, and **26** in the presence of 2M HCl in diethyl ether. The N-alkylated derivatives **5a–f** were subjected to a one-pot reductive amination with benzaldehydes **2a–g** using $NaBH_4$, followed directly by formation of the corresponding ammonium chloride salts (**7**, **9**, **11**, **13**, **14**, **16**, **17**, **19**, **22**, **24**, and **26**) in the presence of 2 M HCl in diethyl ether. All the final compounds were recrystallized to ≥ 95% purity from IPA providing a yield of 31-78%.

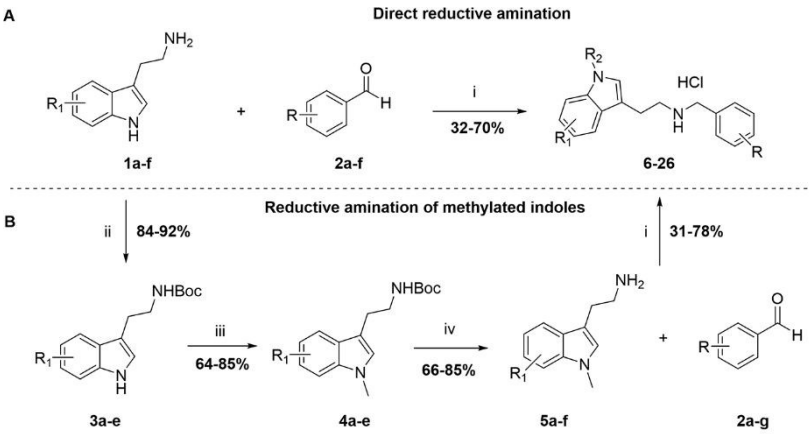

Scheme 1. Synthesis of the indole-based compounds **6**-**26** in sets A-B (Tables 1-2). Reagent and conditions: i) Ethanol or MeOH, rt or reflux, 12h; $NaBH_4$, 0˚C- rt, 5h; 2M HCl in ether; ii) Boc-anhydride, DCM, 0˚C - rt, 12h. iii) NaH, DMF 0˚C- rt; CH_3I, rt, 12h. iv) TFA, DCM 0˚C- rt, 5h. Tryptamines **1a-f** and benzaldehydes **2a-f** can be found in Figures S2-S3.

The compounds in Set C were designed with modifications in the linker (Table 3), which resulted in different synthetic pathways in order to reach the five analogues. The dimethylated compound **30** was accessed in one step from compound **6** in the presence of NaH and CH_3I to form the N,N-dimethyl ammonium iodide salt in a 34% yield (Scheme 2A). The synthesis of the monomethylated analogue **29** is shown in Scheme S2. The three cyclic compounds **31**-**33** were synthesized as racemic mixtures through a one-step Pictet-Spengler reaction of hydrochloric salts of tryptamine derivatives **1d, 5c** with the aldehydes **2a, b** (Scheme 2B). All products of set C, were recrystallized to ≥ 95% purity from IPA after salt formation with a yield of 34-60%.

Table 3. Chemical structures and IC_{50} values of compounds with modified linker in set C.

ID	Structure	*Ag*AChE1 IC_{50} μM[a]	*h*AChE IC_{50} μM[a]	S.R[b]

View Article Online
DOI: 10.1039/D5MD00797F

29	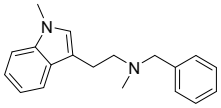	74 (55 - 112)	>500	>7
30	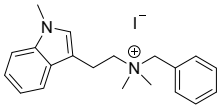	5.5 (3.3 - 6.7)	5.0 (2.0 – 22)	0.9
31	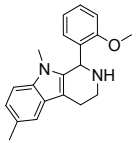	26 (20 - 33)	>500	>19
32	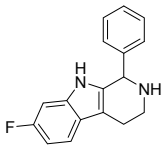	>500	>500	-
33	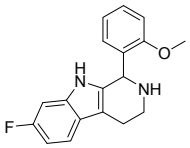	47 (33–78)	> 500	>11

[a]Compounds tested as HCl salts unless specified, values given in parentheses = 95% confidence interval; [b]S.R = selectivity ratios were calculated by taking the compound's IC_{50} for *h*AChE and dividing by its values for *Ag*AChE1.

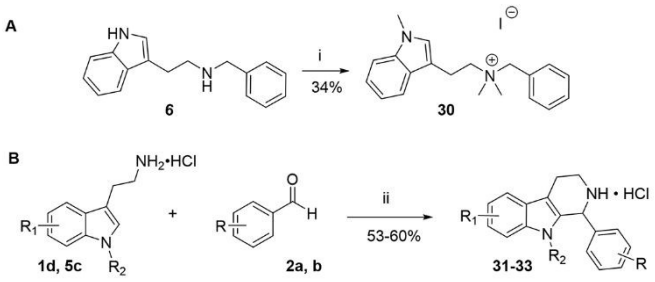

Scheme 2. Synthesis of compounds **30-33** in set C. Reagent and conditions: i) NaH, DMF 0˚C- rt; CH_3I, rt, 12h; ii) Ethanol, reflux, 12h; 2M HCl in ether.

Biochemical evaluation of the indole-based compounds

The synthesized compounds in sets A-C were investigated for their activity against recombinant *Ag*AChE1 and *h*AChE by determination of their half-maximal inhibitory concentrations (IC_{50}) using the Ellman assay (Tables 1-3, Figure S4). Four analogs were also investigated against *Aa*AChE1 (Table 1), which showed a similar inhibition potency with a Pearson correlation coefficient (R^2) of 0.99 based on the pIC_{50} values. Previous studies have shown that also inhibitors from other chemical classes had similar in vitro inhibition profiles against *Ag*AChE1 and *Aa*AChE.[14-17] The indole-based compounds were observed to be potent

View Article Online
DOI: 10.1039/D5MD00797F

inhibitors against *Ag*AChE1, while still having a wide range of IC_{50} values, from 0.04 µM (**16**) up to >500 µM (**36**). Out of the 26 compounds of all three sets, three (**9**, **16**, and **19**) compounds had a good inhibition potency with IC_{50} values between 40 and 70 nM. In addition, five more compounds had IC_{50} values in sub-micromolar range, and only seven inhibitors had IC_{50} values ≥ 20 µM. In case of *h*AChE, the compounds were less active; only three compounds had IC_{50} values below 5.0 µM, and 17 compounds had IC_{50} values ≥ 20 µM. From a selectivity point of view, six compounds were potent and displayed selectivity against *Ag*AChE1 over *h*AChE with selectivity ratios (SR) between 40 and 394 (Tables 1-2). Among these potent and selective inhibitors, **8**, **15**, **16**, and **18** from sets A-B are displayed in the Figure 4.

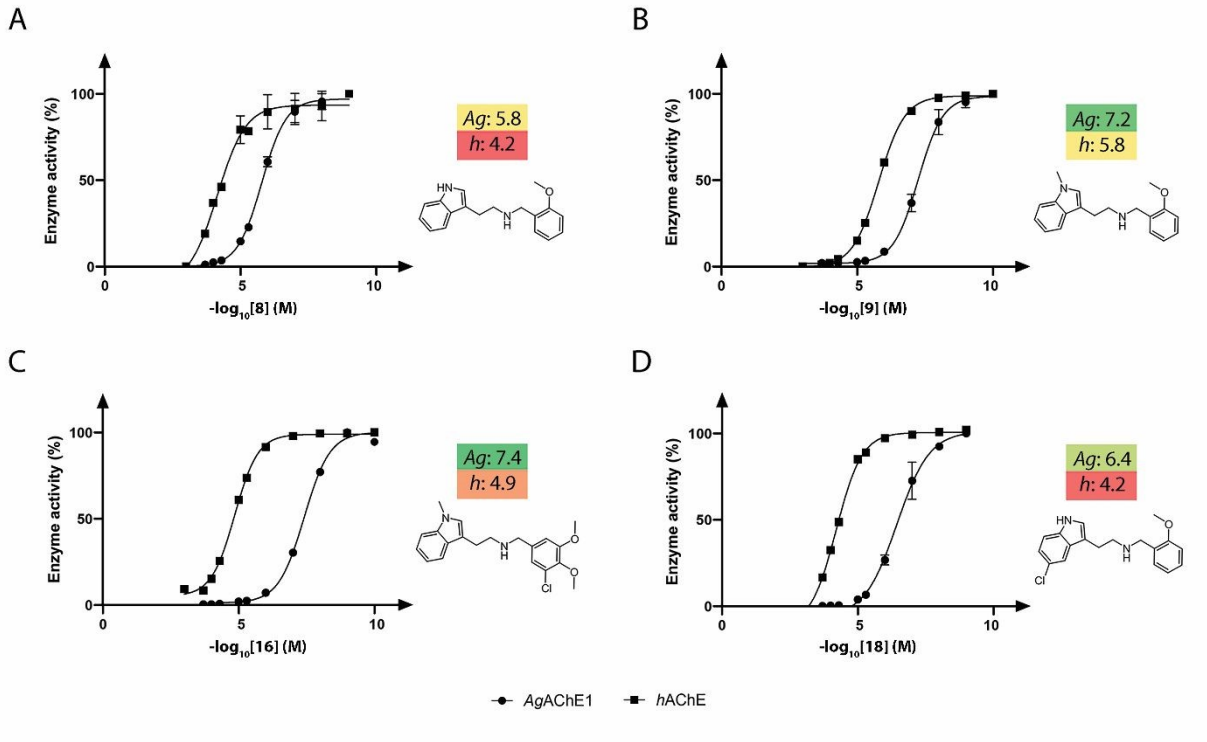

Figure 4. Dose-response curves showing the inhibitory potency of compounds **8** (**A**), **9** (**B**), **16** (**C**), and **18** (**D**) against *Ag*AChE1 (dots) and *h*AChE (squares). The pIC_{50} values are given beside the dose-response curves and are color coded, with dark green, yellow, and dark red indicating the strongest, medium, and weakest inhibitors, respectively.

Structure-activity relationship of inhibition of AChE by the indole-based compounds

Comparison of the IC_{50} values against *Ag*AChE1 for the five pairs of N-H and N-Me indole analogues in set A showed that all compounds increased in potency upon N-methylation of the indole moiety (Table 1), ranging from a 3-fold to almost a 30-fold increase in potency. The increase in potency upon N-methylation was dependent on the benzyl group attached. The unsubstituted **7** gained the least and the ortho methoxy substituted **9** increased potency the most, in comparison to their N-H analogues (**7** vs. **6**, and **9** vs. **8**). Expansion of the pairwise analysis (N-H vs. N-Me) to the analogues in set B showed that also the substituted indole analogues increased their potency against *Ag*AChE1 upon N-methylation of the indole. The methoxy substituted indole derivative increased in potency the most (15-fold) from an IC_{50} value of 48 µM for the N-H analogue **23** to 3.2 µM for the N-Me inhibitor **24** (Table 1). The increase in inhibition potency upon N-methylation of the indole derivatives was not *Ag*AChE1

View Article Online
DOI: 10.1039/D5MD00797F

specific, since also the IC_{50} values against *h*AChE decreased to a similar extent as for the mosquito enzyme (Tables 1-2, Figure 4A-B).

SAR analysis of the modifications of the benzyl moieties in set A showed that different substituents were tolerated with good inhibition potency against *Ag*AChE1. For example, the ortho methoxy- and para nitro substituted benzyl analogues **9** and **11** had both sub-micromolar IC_{50} values. The unsubstituted phenyl ring or non-polar substituents at the para position of the ring appeared to be unfavorable for inhibition of *Ag*AChE1. Interestingly, the inhibitors that contained the bulkiest benzyl moiety, the 3-chloro-4,5-dimethoxybenzyl analogues **15** (N-H) and **16** (N-Me), showed remarkable selectivity for *Ag*AChE1 over *h*AChE with selectivity ratios (S.R.) of 394 and 350, respectively (Figure 4C).

In general, the substitutions at the 5 and 6 positions of the indole moiety of compounds in set B resulted in maintained or decreased inhibition activity against *Ag*AChE1, where the 5-chloro- and 6-fluoro indole analogues gave the best results with low IC_{50} values (Table 2). Still, the 5-chloro N-H indole derivative **18** resulted in improved potency (IC_{50}=0.4 µM) compared to the unsubstituted analogue **8** (IC_{50}=1.6 µM). For the indole part of the molecule, polar substituents such as hydroxyl or methoxy appeared to be less favorable for inhibition activity. Again, an interesting observation was made regarding selectivity for *Ag*AChE1 over *h*AChE. The introduced 5-chloro substituent in the indole moiety did not only improve inhibition potency against *Ag*AChE1 (cf. **18** vs. **8**), it also increased the selectivity for *Ag*AChE1 over *h*AChE, with S.R. of 155 compared to 44 (Figure 4A and D). A similar trend was also seen for the N-Me analogues **19** (5-Cl) and **9** (5-H), with S.R. of 61 and 27, respectively.

The ring closure through bond formation between the benzylic carbon and the carbon at position 2 of the indole yielded conformationally restricted analogues of compounds in set B (set C, Table 3). This modification drastically decreased the inhibitory activity, as seen when comparing the cyclized 6-F analogue **33** with the linear 6-F analogue **21** (IC_{50} values of 47 µM vs. 1.6 µM). This observation was further strengthened when comparing **31** with **20**; despite being N-methylated on the indole, the cyclic **31** showed a 10-fold weaker potency than its N-H linear analogue **20**. Monomethylation of the secondary amine of the linker (**29**) resulted in a moderate loss of inhibitory potency compared to analogue **7**. Converting **7** (IC_{50}=11 µM) to the dimethylated quaternary ammonium analogue **30** resulted in a comparable IC_{50} value of 5.5 µM against *Ag*AChE1. This modification led to a complete loss of selectivity for *Ag*AChE1 over *h*AChE, as the introduction of the permanently charged cation in **30** resulted in an IC_{50} value of 5.0 µM against *h*AChE.

Structure-based analysis of inhibitors in complex with *m*AChE and *Ag*AChE1

Using X-ray crystallography, the two 2-methoxybenzyl analogues **8** (N-H) and **9** (N-Me) were structurally determined in complex with *m*AChE (*m*AChE•**8** and *m*AChE•**9**; PDB: 9SND and 9SNJ). The data of the two complexes was of good quality, with resolutions extending to 2.4 Å and 2.3 Å for *m*AChE•**8** and *m*AChE•**9**, respectively (Table S3). The 3D-structures reveal that both compounds bind at the bottom of the gorge, close to the indole of Trp86, with highly similar biding poses (Figure 5A). The inhibitors have an internal parallel displaced stacking interaction between the phenyl- and indole rings with an arene-arene distance of approximately 4 Å, which resulted in a folded compact binding pose. This binding pose is not possible to obtain for the cyclized compounds in set C (**31**-**33**), which may explain the substantial decrease in potency of these analogues. Furthermore, the two compounds with mono- and dimethylated secondary amines in the linker (**29**-**30**) have presumable different

View Article Online
DOI: 10.1039/D5MD00797F

binding poses compared to the compounds in sets A-B, since also these two would not be able to achieve such compact binding pose without substantial bond strain.

The inhibitors' binding poses have a high shape complementarity with CAS of *m*AChE, where several amino acid residue-inhibitor contacts are observed (Figure 5B-C). The 2-methoxybenzyl moieties of **8** and **9** have parallel displaced arene-arene interactions with $Tyr337_m$, and edge to face arene-arene interactions with $Phe338_m$. Furthermore, the indole moieties of **8** and **9** form face arene contacts with the mainchains of $Gly120_m$ and $Gly121_m$. Although *m*AChE•**8** and *m*AChE•**9** are structurally very similar, there are distinct differences when studying the water molecules in CAS. *m*AChE•**8** has two water molecules that interact with **8** (Figure 5B), while *m*AChE•**9** only have one inhibitor-interacting water molecule (Figure 5C). The water molecule in common by the two complexes has hydrogen bonding distances to the secondary amine in the linker and two amino acid residues, $Thr83_m$ and $Asp74_m$. The unique water molecule in *m*AChE•**8** can form a putative hydrogen bond with N-H in the indole and bridge an interaction to Glu202. The N-methylation of the indole of **9** displaces the water molecule in the *m*AChE•**9** crystal structure compared to *m*AChE•**8**. This difference allows the N-methyl group of **9** to interact with Trp86, which is missing in *m*AChE•**8**. The additional interaction together with the displacement of the water molecule may account for the substantial increased inhibitory activity of the N-Me indole-based inhibitors compared to their N-H analogues.

*Ag*AChE1 has been shown to have a different shape of the gorge compared to *m*AChE, partly due to structurally different placement of the α-helix lining the gorge.[13] $Tyr337_m$ and $Phe338_m$ are located in this α-helix, wherefore the interaction patterns of the inhibitors in complex with *Ag*AChE1 may differ compared to the determined crystal structures. We therefore performed MD simulations of *m*AChE•**9** and *Ag*AChE1•**9** to elucidate the selectivity profile of the indole-based inhibitor **9**.

View Article Online
DOI: 10.1039/D5MD00797F

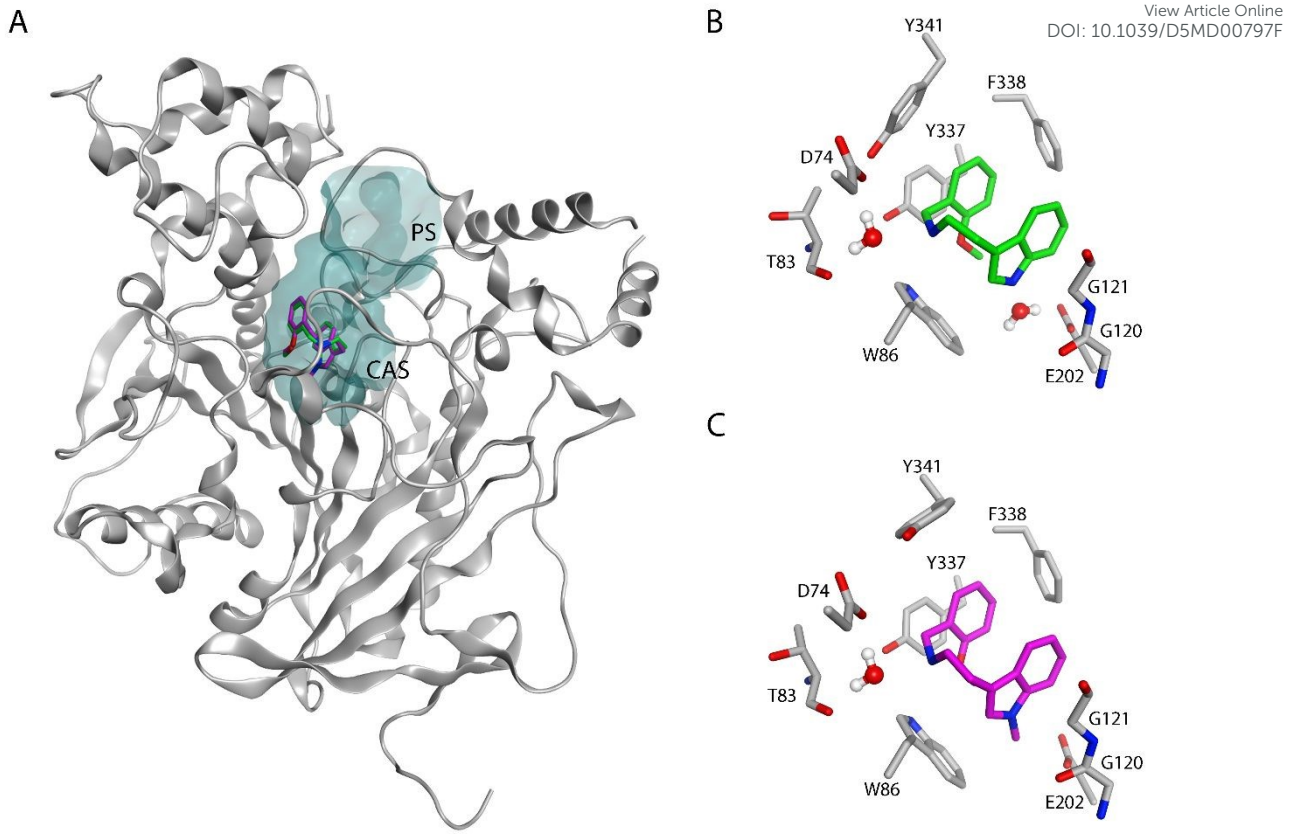

Figure 5. Binding poses of the 2-methoxybenzyl analogues **8** (N-H, green) and **9** (N-Me, magenta) in *m*AChE based on the crystal structures *m*AChE•**8** and *m*AChE•**9** (PDB: 9SND and 9SNJ). (**A**) An overview showing the similar binding poses of **8** and **9** located at the bottom of the active site gorge. (**B**) The binding pose of **8** (N-H, green) with near amino acid residues and two interacting water molecules. (**C**) The binding pose of **9** (N-Me, magenta) with near amino acid residues and one interacting water molecule. The active site gorge is displayed in grey. Hydrogen atoms have been manually added to the oxygen of waters for illustrative purposes.

Five 100 ns MD simulations were performed for *m*AChE•**9** and a prepared model of *Ag*AChE1•**9**, respectively, with varying initial velocities. According to root-mean-square deviation (RMSD) values the simulations obtained convergence after 50 ns (Figure S5). Thus, analysis was performed for the concatenated 50-100 ns simulations. A cluster analysis was performed for the inhibitor conformations over the simulation time, resulting in four and five representative binding modes for *m*AChE•**9** and *Ag*AChE1•**9**, respectively (Figures S6-S9). The three largest clusters accounted for 86% and 84% of the analyzed trajectory for *m*AChE•**9** and *Ag*AChE1•**9**, respectively, and their centroid binding poses are shown in Figure 6.

For *m*AChE•**9**, the compact binding pose at the bottom of the gorge observed for **9** in the X-ray structure was maintained throughout the main part of the simulation (Figure 6A-B). However, the arene-arene interactions between the methoxy benzyl moiety were occasionally formed to $Tyr341_m$ rather than $Tyr337_m$ or $Phe338_m$ (Figure 6A). Furthermore, $Trp86_m$ was flexible over the simulation time (RMSF = 2.1 Å), and sporadic interactions were formed with the indole of **9** (Figures 6A-C). For *Ag*AChE1•**9**, a similar inhibitor conformation was observed over time with some significant differences in the interaction patterns (Figures 6D-F and S10). $Trp245_{Ag}$ was less flexible compared to $Trp86_m$ (RMSF = 0.92 Å) resulting in a more prominent interaction with the indole of **9**. Further, the arene-arene interaction between the methoxy benzyl moiety and $Tyr493_{Ag}$ was more populated compared to *m*AChE ($Tyr341_m$). The face

View Article Online
DOI: 10.1039/D5MD00797F

arene contacts between the indole moiety of **9** and the mainchain of $Gly278_{ag}$/$Gly120_m$ and $Gly279_{ag}$/$Gly121_m$ were observed in both *m*AChE and *Ag*AChE1, although **9** was positioned closer to these residues in complex with *Ag*AChE1, possibly indicating a more favorable interaction. Overall, **9** had closer contacts to amino acid residues in CAS of *Ag*AChE1 during the MD-simulations, compared to the simulations of *m*AChE•**9**.

The occupancy of water molecules within hydrogen bonding distance to the atoms of **9** (heavy atom distance of < 3 Å) was monitored over the simulations of *m*AChE•**9** and *Ag*AChE1•**9** (Table S4). The analysis revealed low populations of water molecules close to the methoxy benzyl- or indole moieties for both complexes, less than 0.2 waters on average, indicating that the aromatic moieties of the inhibitor are highly shielded in the CAS. The positively charged nitrogen in the linker on the other hand, had a higher occupancy of water molecules within 3Å. Here, *m*AChE•**9** displayed a higher water occupancy compared to *Ag*AChE1•**9** (0.9 vs. 0.4), which may be due to the less tight binding mode of the former complex allowing for closer water contacts.

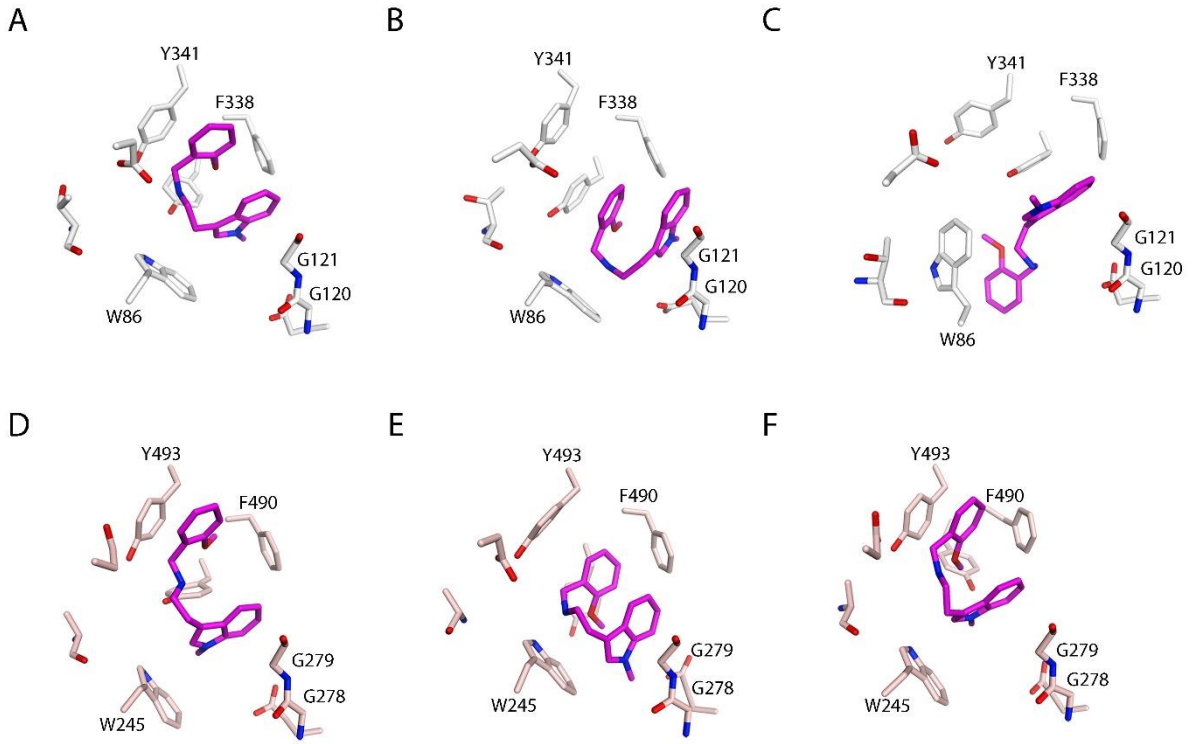

Figure 6. Representative binding poses of **9** in complex with *m*AChE (**A-C**) and *Ag*AChE1 (**D-F**) selected based on cluster analysis of the inhibitors' conformations during the MD-simulations. (**A-C**) The centroid inhibitor conformations of the three largest clusters of *m*AChE•**9** with populations of 40%, 26% and 20% of the analyzed trajectory. (**D-F**) The centroid inhibitor conformations of the three largest clusters of *Ag*AChE•**9** with populations of 35%, 25% and 24% of the analyzed trajectory. Amino acid residues identified as important for interactions with **9** are highlighted. The tyrosine residue in the center of the residues is Y337/Y489.

Insecticidal effects of the indole-based inhibitors

The insecticidal effect of selected indole-based compounds was investigated against female mosquitoes of the species *Ae. aegypti* and *An. gambiae* (Figures 4 and 7, Tables S5-S8). The molecular pair of N-H and N-Me indoles with the 2-methoxy-substituted benzyl (**8** and **9**) was selected to investigate potential in vivo differences of the N-methylation of the indole moiety, and tested at five doses against *Ae. aegypti* (0.02, 0.2, 0.5, 1, and 2 nmol/mosquito, Figure

View Article Online
DOI: 10.1039/D5MD00797F

7A). The N-Me indole analogue **9** had an almost 30-fold better in in vitro inhibitory potency compared to the non-methylated **8** (IC_{50} of 60 nM vs. 1600 nM), and a S.R. of 27. Further, two additional compounds were selected; the highly selective inhibitor the 3-chloro-4,5-dimethoxybenzyl analogue **16** (N-Me, S.R.=350) with an IC_{50} value of 40 nM against *Ag*AChE1, and the selective 5-chloro indole analogue **18** (N-H, S.R.=155) with 10-fold lower inhibitory potency. Compounds **16** and **18** were tested at two doses against both *Ae. aegypti* and *An. gambiae* (0.2 and 2 nmol/mosquito, Figure 7B).

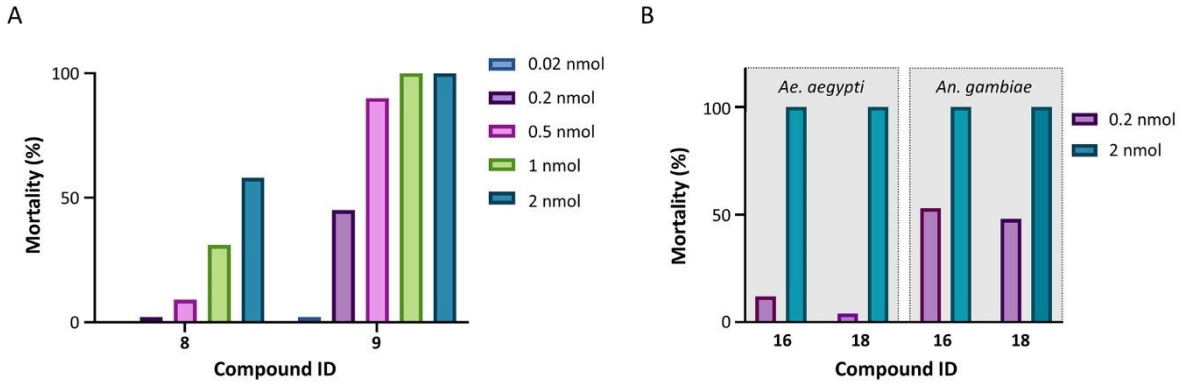

Figure 7. Insecticidal effects of the indole-compounds against mosquitoes using topical application. (**A**) The insecticidal effect of **8** (N-H), and **9** (N-Me) against mosquitoes of the species *Ae. aegypti* at five doses (0.02, 0.2, 0.5, 1, and 2 nmol/mosquito). (**B**) The insecticidal effect of **16** and **18** against both mosquito species *Ae. aegypti*, and *An. gambiae* at doses of 0.2 and 2 nmol/mosquito.

The inhibitors **8** and **9** showed both a clear dose-dependent mortality effect against *Ae. aegypti* (Figure 7A), with approximately a 5-fold stronger insecticidal effect with **9** compared to **8**. The in vivo results of **16** and **18** against *Ae. aegypti* showed that both compounds had 100% mortality at the highest dose, but less effect with the dose of 0.2 nmol/mosquito (Figure 7B), resulting in an intermediate insecticidal effect between **9** and **8**. The topical application of **16** and **18** on *An. gambiae* resulted in a higher insecticidal effect compared to *Ae. aegypti*, which have been observed before.[15, 30, 31] Both compounds showed approximately 50% mortality at the lower dose of 0.2 nmol/mosquito. The observed insecticidal effects were significantly better than previously tested noncovalent AChE1 inhibitors,[15-17] where compound **9** had an approximate LD_{50} of 59 ng/mosquito against *Ae. aegypti* compared to the best insecticidal activity of 4-thiazolidinones of an approximate LD_{50} of 300 ng/mosquito.[17] The results further suggest that there is not a clear relation between in vitro potency against *Ag*AChE1 and in vivo effect. The nanomolar in vitro potency was expected to result in an even stronger insecticidal effect; the currently used insecticides propoxur and bendiocarb have reported LD_{50} values of 5.4 ng and 1.8 ng per mosquito.[32] This discrepancy has been reported before,[15-17] and may be accounted to the physicochemical properties of the inhibitors. For example, the number of hydrogen bond donors have been proposed to be critical, and should be kept low for a successful insecticide.[33, 34] Thus, the secondary amine of the linker may contribute to the lower in vivo insecticidal activity than expected.

Conclusion

There is a need for new active ingredients to be used as insecticides in vector control of disease-transmitting mosquitoes. Here, indole-based hit compounds from a previous HTS were confirmed as potent and selective inhibitors against AChE1s from the vectors *An.*

View Article Online
DOI: 10.1039/D5MD00797F

gambiae and *Ae. aegypti* that spread infectious diseases like malaria and dengue. Three sets of molecules were designed and synthesized to explore the three parts of the molecule, (A) the benzyl-, (B) the indole- and (C) the linker moieties. Methylation of the indole moiety increased the inhibitory potency for all investigated compounds. The most potent compounds **9**, **16** and **19** had IC_{50} values of 40-70 nM against *Ag*AChE1 and were selective over *h*AChE. The bulkiest benzyl derivatives **15** and **16** proved to be highly selective for *Ag*AChE1 over *h*AChE with S.R. of 394 and 350. Compound **9** had a strong in vivo insecticidal activity with an approximate LD_{50} of 59 ng per mosquito of species *Ae. aegypti*, which is a 5-fold improvement of previous noncovalent AChE1 inhibitors although still less potent than currently used insecticides. Crystal structures of *m*AChE•**8** and *m*AChE•**9** showed that the inhibitors form a compact folded binding pose in the lower part of the active site gorge, which could explain the drastic loss of activity of the cyclic derivatives in set C. MD simulations revealed that **9** had closer amino acid residue contacts in *Ag*AChE compared to *m*AChE, in particular between the tryptophan residue in CAS and the indole ring of **9**. The binding pose analysis opens up for further medicinal chemistry optimizations of the indole inhibitors to improve their in vivo insecticidal activity.

Experimental section

General aspects of synthesis of indole-based compounds

All commercially available reagents and solvents were purchased from Enamines, Sigma-Aldrich, Fluorochem, and Fisher Scientific with ≥ 95% purity, and used without further purification. TLC aluminium sheets coated with silica gel, were purchased from Merck. The DMF was dried in a solvent drying system (Glass Contour Solvent Systems, SG Water USA), and stored in sealed RBF, containing 4 Å molecular sieves activated at 180 °C in the oven for more than 48 h before use. All the reactions were carried out under an inert atmosphere in the presence of N_2 gas. The reaction progress rates were monitored by TLC spot visualization by UV detection (254 nm) or by staining with ninhydrin solution, and with LC-MS (6130 Quadrupole (Agilent Technologies, USA) mass spectrometer connected to an Agilent 1260 Infinity LC system) analysis. Synthesized compounds were purified with flash column chromatography (eluents given in brackets) were performed on normal phase silica gel (Merck, 60 Å, 40-63 µm), and on Biotage Isolera One automated flash chromatography system using Biotage® Sfär Silica, Duo 60 µm silica gel disposable cartridges. Some hydrochloric salt compounds were purified using the crystallization technique with IPA. High-resolution mass spectrometry (HRMS) data was obtained on Agilent Technologies 6230 TOF LC/MS in ESI mode. NMR spectra were acquired on a Bruker DRX 400 or 600 MHz instrument at 298K unless otherwise stated. The δ values were referenced to the residual solvent signals of $CDCl_3$ (7.26 ppm), DMSO-d_6 (2.50 ppm), or CD_3OD (3.31 ppm) as internal standards for ^1H, and $CDCl_3$ (77.16 ppm), DMSO-d_6 (39.52 ppm), or CD_3OD (49.00 ppm) for ^{13}C. The following abbreviations were used to assign the NMR peaks; s = singlet, d = doublet, t = triplet, q = quartet, bs = broad singlet, dd = doublet of doublets, dt = double of triplets, m = multiplet. Target compounds were ≥ 95% pure according to $^1H/^{13}C$ NMR data and LC–MS UV traces.

Synthesis of building blocks

General procedure for the synthesis of 3a-e.

View Article Online
DOI: 10.1039/D5MD00797F

The corresponding indoles **1a-f** (1 eq) were dissolved in DCM (2.4 ml/mmol), then TEA (1.5 eq) and di-tert-butyl dicarbonate (1-1.1 eq) were added at rt and the mixture was stirred for 12 h. After completion of the reaction, the reaction was quenched by the addition of water (50 ml), and extracted with 2×150 ml DCM. The combined organic layers were washed with an aqueous saturated $NaHCO_3$ solution, and brine. The organic phase was finally dried over Na_2SO_4, filtered, and concentrated to obtain the crude compound without further purification.

Tert-butyl (2-(1H-indol-3-yl)ethyl)carbamate (3a). 2-(1H-indol-3-yl)ethan-1-amine **1a** (2.0 g, 12.4 mmol) was dissolved in DCM (2.4 ml/mmol) followed by the addition of TEA (2.6 ml, 18.7 mmol) at rt. Di-tert-butyl dicarbonate (3.0 g, 13.7 mmol) was then added, and the reaction followed the general procedure. The desired product **3a** was obtained as a brown powder (3.0 g, 92% yield). ^{1}H NMR (400 MHz, $CDCl_3$) δ 8.01 (bs, 1H), 7.61 (d, 1H, *J* = 8.8 Hz), 7.38 (d, 1H, *J* = 8.0 Hz), 7.23-7.18 (m, 1H), 7.15-7.10 (m, 1H), 7.00 (s, 1H), 4.62 (bs, 1H), 3.46 (t, 2H, *J* = 7.0 Hz), 2.96 (t, 2H, *J* = 6.8 Hz), 1.43 (s, 9H); ^{13}C NMR (100 MHz, $CDCl_3$) δ 156.1, 136.5, 122.3 (2C), 122.1, 119.6 (2C), 119.0, 111.3, 77.3, 41.0, 28.6 (3C), 25.4.

Tert-butyl (2-(5-chloro-1H-indol-3-yl)ethyl)carbamate (3b). 2-(5-chloro-1H-indol-3-yl)ethan-1-amine **1b** (1.2 g, 5.25 mmol) was dissolved in DCM (2.4 ml/mmol) followed by the addition of TEA (1.1 ml, 7.88 mmol) at rt. Di-tert-butyl dicarbonate (1.26 g, 5.78 mmol) was then added, and the reaction followed the general procedure. The desired product **3b** was obtained as a brown powder (1.4 g, 90% yield). ^{1}H NMR (400 MHz, $CDCl_3$) δ 8.10 (bs, 1H), 7.53-7.52 (m, 1H), 7.24 (d, 1H, *J* = 2.8 Hz), 7.12 (d, 1H, *J* = 8.8 Hz), 7.03 (s, 1H), 4.63 (bs, 1H), 3.40 (t, 2H, *J* = 6.8 Hz), 2.88 (t, 2H, *J* = 6.8 Hz), 1.41 (s, 9H); ^{13}C NMR (100 MHz, $CDCl_3$) δ156.3, 134.8, 128.7 125.4, 123.6, 122.6, 118.5, 113.3, 112.3, 77.4, 41.2, 28.6 (3C), 25.9.

Tert-butyl (2-(5-methyl-1H-indol-3-yl)ethyl)carbamate (3c). 2-(5-methyl-1H-indol-3-yl)ethan-1-amine **1c** (0.3 g, 1.42 mmol) was dissolved in DCM (2.4 ml/mmol) followed by the addition of TEA (0.29 ml, 2.13 mmol) at rt. Di-tert-butyl dicarbonate (0.34 g, 1.56 mmol) was then added, and the reaction followed the general procedure. The desired product **3c** was obtained as light brown solid (0.35 g, 90% yield). ^{1}H NMR (400 MHz, $CDCl_3$) δ 7.93 (bs, 1H), 7.39 (s, 1H), 7.27-7.25 (m, 1H), 7.04-7.01 (m, 1H), 7.00 (s, 1H), 4.61 (bs, 1H), 3.45 (t, 2H, *J* = 7.2 Hz), 2.93 (t, 2H, *J* = 6.6 Hz), 2.46 (s, 3H), 1.43 (s, 9H); ^{13}C (150 MHz, $CDCl_3$) δ 156.1, 134.9, 128.8, 127.8, 123.9, 122.3, 118.6, 112.8, 111.0, 79.2, 41.1, 28.6 (3 C), 25.9, 21.6.

Tert-butyl (2-(6-fluoro-1H-indol-3-yl)ethyl)carbamate (3d). 2-(6-fluoro-1H-indol-3-yl)ethan-1-amine **1d** (0.2 g, 1.20 mmol) was dissolved in DCM (2.4 ml/mmol) followed by the addition of TEA (0.25 ml, 1.80 mmol) at rt. Di-tert-butyl dicarbonate (0.26 g, 1.20 mmol) was then added, and the reaction followed the general procedure. The desired product **3d** was obtained as a brown solid (0.25 mg, 75% yield). ^{1}H NMR (400 MHz, $CDCl_3$) δ 8.15 (bs, 1H), 7.51-7.47 (m, 1H), 7.06-7.02 (m, 1H), 7.00 (s, 1H), 6.91-6.85 (m, 1H), 4.62 (bs, 1H), 3.44 (t, 2H, *J* = 6.8 Hz), 2.92 (t, 2H, *J* = 7.0 Hz), 1.44 (s, 9H); ^{13}C NMR (100 MHz, $CDCl_3$) δ 160.5 (d, *J* 1-*C*-*F* = 227 Hz), 156.2, 136.4 (d, *J* 3-C-F = 12 Hz), 124.1, 122.3 (d, *J* 4-*C*-*F* = 3.5 Hz), 119.6 (d, *J* 3-C-F = 10 Hz), 113.4, 108.3 (d, *J* 2-C-F = 26 Hz), 95.6 (d, *J* 2-C-F = 26 Hz), 79.7, 41.2, 28.6 (3C), 26.0.

Tert-butyl (2-(5-methoxy-1H-indol-3-yl)ethyl)carbamate (3e). 2-(5-methoxy-1H-indol-3-yl)ethan-1-amine **1e** (1.0 g, 5.25 mmol) was dissolved in DCM (2.4 ml/mmol) followed by the addition of TEA (1.1 ml, 7.88 mmol) at rt. Di-tert-butyl dicarbonate (1.3 g, 5.78 mmol) was then added, and reaction followed the general procedure. The desired product **3e** was obtained as a brown solid (1.3 g, 85% yield). ^{1}H NMR (400 MHz, $CDCl_3$) δ 8.08 (bs, 1H), 7.26-7.24 (m, 1H),

View Article Online
DOI: 10.1039/D5MD00797F

7.03 (d, 1H, *J* = 2.4 Hz) 7.00 (s, 1H), 6.86 (dd, 1H, *J* 1 = 8.8 Hz, *J* 2 = 2.4 Hz), 4.61 (bs, 1H), 3.87 (s, 3H), 3.45 (t, 2H, *J* = 6.8 Hz), 2.92 (t, 2H, *J* = 7.2 Hz), 1.44 (s, 9H); ^{13}C NMR (100 MHz, $CDCl_3$) δ 156.4, 154.1, 131.7, 127.9, 123.0, 112.9, 112.4, 112.1, 100.7, 79.6, 56.1, 41.3, 28.5 (3C), 26.0.

General procedure for the synthesis of 4a-e.
NaH 60% in mineral oil (1.1 eq) was dissolved in dry DMF (1.2 ml/mmol). The corresponding carbamates **3a-e** (1.0 eq) were dissolved in dry DMF (2.5 ml/mmol) and added with syringe at 0°C into the NaH solution. After the addition the reaction was stirred for 30 minutes at rt. CH_3I (1.1 eq) was then dropwise added to the mixture at 0°C, and allowed to stir at rt for 12 hours. After completion, the residue was dissolved in H_2O (200 ml) and extracted with 3×150 ml EtOAc. The combined organic layers were washed with brine and dried over Na_2SO_4, filtered, and concentrated to afford an oil as a crude. The purification over column chromatography using EtOAc:heptane (50:50) or MeOH:DCM:TEA (10:89:1) gave the corresponding methylated indoles **4a-e**.

Tert-butyl(2-(1-methyl-1H-indol-3-yl)ethyl)carbamate (4a). NaH 60% in mineral oil (0.5 g, 12.6 mmol) was dissolved in dry DMF (1.2 ml/mmol). Tert-butyl (2-(1H-indol-3-yl)ethyl)carbamate **3a** (3.0 g, 11.5 mmol) was also dissolved in dry DMF (2.5 ml/mmol) and added at 0°C into the NaH solution. After the addition the reaction was stirred for 30 minutes at rt. CH_3I (1.7 g, 12.6 mmol) was added, and the reaction followed the general procedure. The crude was obtained as a brown oil, then purified over column chromatography using EtOAc:heptane (50:50) to provide **4a** (2.7 g, 85% yield). ^{1}H NMR (400 MHz, $CDCl_3$) δ 7.59 (d, 1H, *J* = 7.6 Hz), 7.30 (d, 1H, *J* = 7.6 Hz), 7.25-7.21 (m, 1H), 7.13-7.09 (m, 1H), 6.89 (s, 1H), 4.59 (bs, 1H), 3.76 (s, 3H), 3.44 (t, 2H, *J* = 6.8 Hz), 2.94 (t, 2H, *J* = 7.0 Hz), 1.44 (s, 9H); ^{13}C NMR (100 MHz, $CDCl_3$) δ 156.1, 137.2, 128.0, 127.0, 121.8 (2C), 119.1, 119.0 111.7, 109.4, 79.2, 41.3, 32.8, 28.6 (3C), 25.9.

Tert-butyl (2-(5-chloro-1-methyl-1H-indol-3-yl)ethyl)carbamate (4b). NaH 60% in mineral oil (0.18 g, 4.66 mmol) was dissolved in dry DMF (1.2 ml/mmol). Tert-butyl (2-(5-chloro-1H-indol-3-yl)ethyl)carbamate **3b** (1.25 g, 4.24 mmol) was also dissolved in dry DMF (2.5 ml/mmol) and added at 0°C into the NaH solution. After the addition the reaction was stirred for 30 minutes at rt. CH_3I (0.66 g, 4.66 mmol) was added, and the reaction followed the general procedure. The crude was obtained as a yellow oil, then purified over column chromatography using MeOH:DCM:TEA (10:89:1) to provide **4b** (0.87 g, 67% yield). ^{1}H NMR (400 MHz, $CDCl_3$) δ 7.53 (d, 1H, *J* = 1.6 Hz), 7.21-7.15 (m, 2H), 6.91 (bs, 1H), 4.65 (bs, 1H), 3.74 (s, 3H), 3.41 (t, 2H, *J* = 6.8 Hz), 2.89 (t, 2H, *J* = 6.8 Hz), 1.43 (s, 9H); ^{13}C NMR (100 MHz, $CDCl_3$) δ 163.2, 135.7, 128.4, 125.0 (2 C), 122.1 (2C), 118.5, 110.4 (2C), 77.3, 41.4, 33.0, 28.5 (3C), 25.8.

Tert-butyl (2-(1,5-dimethyl-1H-indol-3-yl)ethyl)carbamate (4c). NaH 60% in mineral oil (0.07 g, 1.28 mmol) was dissolved in dry DMF (1.2 ml/mmol). Tert-butyl (2-(5-methyl-1H-indol-3-yl)ethyl)carbamate **3c** (0.32 g, 1.16 mmol) was also dissolved in dry DMF (2.5 ml/mmol) and added at 0°C into the NaH solution. After the addition the reaction was stirred for 30 minutes at rt. CH_3I (0.48 g, 1.28 mmol) was added, and the reaction followed the general procedure. The crude was obtained as a yellow oil, then purified over EtOAc:heptane (50:50) to provide **4c** (0.3 g, 89% yield). ^{1}H NMR (400 MHz, $CDCl_3$) δ 7.36 (s, 1H), 7.18 (d, 1H, *J* = 8.0 Hz), 7.05 (dd, 1H, *J* 1 = 7.6 Hz, *J* 2 = 1.6 Hz), 6.84 (s, 1H), 4.60 (bs, 1H), 3.72 (s, 3H), 3.43 (t, 2H, *J* = 6.8 Hz), 2.91 (t, 2H, *J* = 6.4 Hz), 2.46 (s, 3H), 1.44 (s, 9H); ^{13}C NMR (100 MHz, $CDCl_3$) δ 156.1, 135.7, 128.2, 127.1, 123.4 (2C), 118.7, 111.1, 109.1, 79.1, 41.1, 32.8, 28.6 (3C), 25.8, 21.6.

View Article Online
DOI: 10.1039/D5MD00797F

Tert-butyl (2-(6-fluoro-1-methyl-1H-indol-3-yl)ethyl)carbamate (4d). NaH 60% in mineral oil (0.03 g, 0.75 mmol) was dissolved in dry DMF (1.2 ml/mmol). Tert-butyl (2-(6-fluoro-1H-indol-3-yl)ethyl)carbamate **3d** (0.14 g, 0.50 mmol) was also dissolved in dry DMF (2.5 ml/mmol) and added at 0°C into the NaH solution. After the addition the reaction was stirred for 30 minutes at rt. CH_3I (0.10 g, 0.75 mmol) was added, and the reaction followed the general procedure. The crude was obtained as a yellow oil, then purified over column chromatography using MeOH:DCM:TEA (10:89:1) to provide **4d** (0.1 g, 68% yield). ^{1}H NMR (400 MHz, $CDCl_3$) δ 7.50-7.46 (m, 1H), 6.95 (dd, 1H, *J* 1 = 10 Hz, *J* 2 = 2.0 Hz), 6.89-6.83 (m, 2H), 4.59 (s, 1H), 3.70 (s, 3H), 3.44-3.41 (m, 2H), 2.91 (t, 2H, *J* = 7.0 Hz), 1.44 (s, 9H); ^{13}C NMR (100 MHz, $CDCl_3$) δ 160.0 (d, *J* 1-*C*-*F* = 243 Hz), 156.0, 137.3 (d, *J* 3-C-F = 10 Hz), 127.1, 124.5, 119.6 (d, *J* 3-C-F = 10 Hz), 112.0, 107.7 (d, *J* 2-C-F = 26 Hz), 95.7 (d, *J* 2-C-F = 26 Hz), 79.3, 41.1, 32.9, 28.5 (3C), 25.9.

Tert-butyl (2-(5-methoxy-1-methyl-1H-indol-3-yl)ethyl)carbamate (4e). NaH 60% in mineral oil (0.25 g, 6.19 mmol) was dissolved in dry DMF (1.2 ml/mmol). Tert-butyl (2-(5-methoxy-1H-indol-3-yl)ethyl)carbamate **3e** (1.2 g, 4.13 mmol) was also dissolved in dry DMF (2.5 ml/mmol) and added at 0°C into the NaH solution. After the addition the reaction was stirred for 30 minutes at rt. CH_3I (1.9 ml, 6.2 mmol) was added, and the reaction followed the general procedure. The crude was obtained as a yellow oil, then purified over column chromatography using MeOH:DCM: TEA (10:89:1) to provide **4e** (1.0 g, 80% yield) ^{1}H NMR (400 MHz, $CDCl_3$) δ 7.20 (d, 1H, *J* = 8.8 Hz), 7.02 (d, 1H, *J* = 2.4 Hz), 6.90-6.83 (m, 2H), 4.74 (bs, 1H), 3.87 (s, 3H), 3.73 (s, 3H), 3.43 (t, 2H, *J* = 6.6 Hz), 2.90 (t, 2H, *J* = 6.6 Hz), 1.43 (s, 9H); ^{13}C NMR (100 MHz, $CDCl_3$) δ 156.2, 153.8, 132.7, 128.2, 127.6, 112.2, 110.2, 110.0, 100.9, 79.4, 56.3, 41.3, 33.0, 28.9 (3C), 26.1.

Tert-butyl methyl(2-(1-methyl-1H-indol-3-yl)ethyl)carbamate (27). NaH 60% in mineral oil (174 mg, 4.37 mmol) was dissolved in dry DMF (1.2 ml/mmol). Compound tert-butyl (2-(1-methyl-1H-indol-3-yl)ethyl)carbamate **4a** (159 mg, 0.54 mmol) was also dissolved in dry DMF (2.5 ml/mmol) and was added slowly into the solution of NaH at 0°C, and reaction was cooled down to 0°C and CH_3I (341 µl, 5.46 mmol) was added dropwise to the reaction, and after completion of addition, the mixture was stirred at rt for 30 minutes, then 5 hours at 80°C. After completion, the crude was dissolved in H_2O (200 ml) and extracted 3×50 ml EtOAc, combined organic layers was washed with brine dried over Na_2SO_4, filtered and concentrated, obtained brown sticky crude was purified over column chromatography EtOAc:heptane (50:50) to provide **27** (100 mg, 63.4% yield). ^{1}H NMR (400 MHz, $CDCl_3$) *inter alia* δ 7.76 (d, 1H, *J* = 8.8 Hz), 7.44 (d, 1H, *J* = 8.0 Hz), 7.40-7.36 (m, 1H), 7.29-7.25 (m, 1H), 7.04-7.00 (m, 1H), 3.88 (s, 3H), 3.64 (m, 2H), 3.10-3.09 (m, 2H), 3.03 (s, 3H), 1.42 (s, 9H); ^{13}C NMR (100 MHz, $CDCl_3$) δ 155.9, 137.2, 126.8 (2C), 121.7, 119.0 118.9, 112.0, 109.3, 79.3, 49.9, 37.5, 34.4, 28.5 (3C) 23.3.

Common procedure for the synthesis of 5a-f. The corresponding carbamates **4a**-**4e** or **27** (1.0 eq) were dissolved in DCM (2.5 ml/mmol), then TFA (30 eq) was added to the reaction mixture at rt and the solution was stirred for 1 h. After completion, the reaction was quenched with a solution of saturated $NaHCO_3$, the aqueous layer was extracted with 3×150 ml DCM, and the combined organic layers were washed with brine and dried over Na_2SO_4, filtered, and concentrated to gave the corresponding methylated indoles **5a-e**.

(2-(1-methyl-1H-indol-3-yl)ethan-1-amine (5a). Tert-butyl (2-(1-methyl-1H-indol-3-yl)ethyl)carbamate **4a** (2.6 g, 9.73 mmol) was dissolved in DCM (2.5 ml/mmol), then TFA (1.9 ml, 25 mmol) was added at rt, and the reaction followed the general procedure. The desired

View Article Online
DOI: 10.1039/D5MD00797F

compound was obtained as a powder **5a** (1.2 g, 71% yield). ^{1}H NMR (400 MHz, DMSO-d_6) δ 8.02 (bs, 3H), 7.58 (d, 1H, *J* = 8.0 Hz), 7.42 (d, 1H, *J* = 8.0 Hz), 7.23 (s, 1H), 7.17 (t, 1H, *J* = 7.6 Hz), 7.06 (t, 1H, *J* = 7.4 Hz), 3.75 (s, 3H), 3.04-3.01 (m, 4H); ^{13}C NMR (100 MHz, DMSO-d_6) δ 136.7, 127.8, 127.1, 121.3, 118.6, 118.4, 109.8, 108.8, 40.6, 32.3, 23.0.

2-(5-chloro-1-methyl-1H-indol-3-yl)ethan-1-amine (5b). Tert-butyl (2-(5-chloro-1-methyl-1H-indol-3-yl)ethyl)carbamate **4b** (0.85 g, 2.75 mmol) dissolved in DCM (2.5 ml/mmol), then TFA (6.3 ml, 82.5 mmol) was added to reaction at rt, and the reaction followed the general procedure. The desired compound was obtained as a brown powder **5b** (0.49 g**,** 85% yield) ^{1}H NMR (400 MHz, $CDCl_3$) δ 7.54 (s, 1H), 7.16 (m, 2H), 6.92 (s, 1H), 3.72 (s, 3H), 3.01 (s, 2H), 2.87 (s, 2H), 2.77 (s, 2H); ^{13}C NMR (100 MHz, $CDCl_3$) δ 135.7, 128.5 (2C), 124.8, 122.0, 118.6, 111.4, 110.4, 42.1, 32.9, 28.2.

2-(1,5-dimethyl-1H-indol-3-yl)ethan-1-amine (5c). Tert-butyl (2-(1,5-dimethyl-1H-indol-3-yl)ethyl)carbamate **4c** (0.29 g, 1.00 mmol) dissolved in DCM (2.5 ml/mmol), then TFA (2.3 ml) was added to reaction at rt, and the reaction followed the general procedure. The desired compound was obtained as a brown powder **5c** (0.17 g, 89% yield). ^{1}H NMR (400 MHz, $CDCl_3$) δ 7.32 (s, 1H), 7.14 (d, 1H, *J* = 8.0 Hz), 7.00 (d, 1H, *J* = 8.4 Hz), 6.88 (bs, 1H), 5.92 (s, 2H), 3.66 (s, 3H), 3.16-3.05 (m, 4H), 2.42 (s, 3H); ^{13}C NMR (100 MHz, $CDCl_3$) δ 135.7, 128.4, 128.1, 127.6, 123.7, 118.3, 109.3, 108.1, 40.5, 32.8, 24.1, 21.5.

2-(6-fluoro-1-methyl-1H-indol-3-yl)ethan-1-amine (5d). Tert-butyl (2-(6-fluoro-1-methyl-1H-indol-3-yl)ethyl)carbamate **5d** (0.12 g, 0.41 mmol) dissolved in DCM (2.5 ml/mmol), then TFA (0.9 ml) was added to reaction at rt, and the reaction followed the general procedure. The desired compound was obtained as a brown powder **5d** (60 mg**,** 76% yield) ^{1}H NMR (400 MHz, DMSO-d_6) δ 7.86 (bs, 2H), 7.57-7.53 (m, 1H), 7.30-7.27 (m, 1H), 7.22 (s, 1H), 6.91 (t, 1H, *J* = 9.0 Hz), 3.72 (s, 3H), 3.07-3.01 (m, 2H), 2-99-2.93 (m, 2H); ^{13}C NMR (100 MHz, DMSO-d_6) δ 159.2 (d, *J* 1-*C-F* = 240 Hz) , 136.8 (d, *J* 3-C-F = 10 Hz), 128.4 (d, *J* 4-C-F = 3.1 Hz), 123.9, 119.5 (d, *J 3*-C-F = 10 Hz), 109.2, 107.0 (d, *J* 2-C-F = 24 Hz), 96.2 (d, *J* 2-C-F = 24 Hz), 48.6, 32.5 , 22.8.

2-(5-methoxy-1-methyl-1H-indol-3-yl)ethan-1-amine (5e). Tert-butyl (2-(5-methoxy-1-methyl-1H-indol-3-yl)ethyl)carbamate **4e** (1.0 g, 3.28 mmol) dissolved in DCM (2.5 ml/mmol), then TFA (7.5 ml) was added to reaction at rt, and the reaction followed the general procedure. The desired compound was obtained as a brown powder **5e** (0.55 g**,** 82% yield). ^{1}H NMR (400 MHz, DMSO-d_6) δ 7.97 (bs, 2H), 7.30 (d, 1H, *J* = 8.8 Hz), 7.16 (s, 1H), 7.08 (d, 1H, *J* = 2.0 Hz), 6.83-6.78 (m, 1H), 3.72 (s, 3H), 3.70 (s, 3H), 3.06-2.91 (m, 4H); ^{13}C NMR (100 MHz, DMSO-d_6) δ 153.3, 132.1, 128.3, 127.5, 111.3, 110.5, 108.3, 100.4, 55.5, 40.1, 32.5, 22.9.

3-(2-aminoethyl)-1-methyl-1H-indol-5-ol (5f). 2-(5-methoxy-1-methyl-1H-indol-3-yl)ethan-1-amine **5e** (0.27 g, 1.32 mmol) dissolved in DCM (2.5 ml/mmol) and allowed to stir and cool down until -70 ^{o}C. After 10 minutes BBr_3 (0.66 g, 2.64 mmol) was added slowly to reaction mixture. After the addition was complete, the reaction was allowed to reach 0°C and stirred for 4 hours. The reaction mixture was diluted with dichloromethane (25 mL), washed with water (2x10 mL) and brine (20 mL), dried over anhydrous Na_2SO_4, and the solvent was removed and purified by column chromatography using 20% ethyl acetate in petroleum ether as the eluent to provide desired compound **5f** as a brown powder (0.24 g, 67% yield). ^{1}H NMR (400 MHz, CD_3OD) δ 7.18 (d, 1H, *J* = 8.8 Hz), 7.07 (s, 1H), 6.97 (d, 1H, *J* = 2.0 Hz), 6.76 (dd, 1H, *J* 1= 8.2 Hz, *J* 2 = 2.6 Hz), 3.73 (s, 3H), 3.20 (t, 2H, *J* = 6.2 Hz), 3.06 (t, 2H, *J* = 6.8 Hz); ^{13}C NMR (100 MHz, CD_3OD) δ 152.0, 133.9, 129.4 (2C), 112.7, 111.2, 108.6, 103.4, 41.0, 32.9, 24.4.

View Article Online
DOI: 10.1039/D5MD00797F

N-methyl-2-(1-methyl-1H-indol-3-yl)ethan-1-amine (28, Scheme S3). Tert-butyl methyl(2-(1-methyl-1H-indol-3-yl)ethyl)carbamate **27** (0.1 g, 0.32 mmol) dissolved in DCM (2.5 ml/mmol), then TFA (0.8 ml) was added to reaction at rt, and the reaction followed the general procedure. The desired compound was obtained as a brown powder **28** (0.05 g**,** 76% yield). ^{1}H NMR (400 MHz, $CDCl_3$) δ 7.59 (d, 1H, *J* = 8.0 Hz), 7.29 (d, 1H, *J* = 8.4 Hz), 7.24 (t, 1H, *J* = 7.6 Hz), 7.11 (t, 1H, *J* = 7.4 Hz), 6.92 (s, 1H), 6.31 (bs, 1H), 3.73 (s, 3H), 3.12-3.09 (m, 4H), 2.54 (s, 3H); ^{13}C NMR (100 MHz, $CDCl_3$) δ 137.2, 127.5, 127.3, 122.0, 119.2, 118.8, 110.1, 109.5, 50.9, 34.4, 32.7, 23.6.

General procedure for synthesis of indoles 6-17

The corresponding tryptamines **5a-f** (1.0 eq) and the corresponding benzaldehydes **2a-f** (1.1 eq) were dissolved in EtOH or MeOH (3 ml/mmol) and allowed to reflux for 12h. The reaction mixture was then cooled down to rt and $NaBH_4$ (1.5 eq) was added and allowed to stirred at rt for 1h. After completion, the reaction was quenched with a saturated solution of $NaHCO_3$ and EtOAc was added. The water phase was extracted three times with EtOAc (3× 150 ml), the combined organic layers were washed once with brine, dried over Na_2SO_4, filtered, and concentrated. The crude was dissolved in EtOAc (1 ml) and treated with 2M HCl (1.0 eq) in diethyl ether at 0°C, filtered, and then recrystallized from IPA to obtain the desired compound as white powder.

N-benzyl-2-(1H-indol-3-yl)ethan-1-amine hydrochloride (6).

2-(1H-indol-3-yl)ethan-1-amine **1a** (150 mg, 0.94 mmol), and benzaldehyde **2a** (109 mg, 1.03 mmol) were dissolved in EtOH (3 ml/mmol) and allowed to reflux at 90°C for 12h. The reaction mixture was cooled down to rt and $NaBH_4$ (53.1 mg, 1.40 mmol) was added, and the reaction was carried out according to the general procedure to afford compound **6** (170 mg, 63% yield). ^{1}H NMR (400 MHz, DMSO-d_6) δ 11.0 (bs, 1H), 9.28 (bs, 2H), 7.58-7.55 (m, 3H), 7.47-7.42 (m, 3H), 7.37 (d, 1H, *J* = 6.8 Hz), 7.24-7.20 (m, 1H), 7.12-6.99 (m, 2H), 4.20 (s, 2H), 3.18-3.13 (m, 4H); ^{13}C NMR (100 MHz, DMSO-d_6) δ 136.3, 132.1, 130.0 (2C), 128.9, 128.7 (2C), 126.7, 123.3, 121.2, 118.5, 118.1, 111.6, 109.3, 49.8, 47.1, 21.6. HRMS m/z $[M+H]^+$ calcd. 251.1543, found 251.1511.

N-benzyl-2-(1-methyl-1H-indol-3-yl)ethan-1-amine hydrochloride (7). 2-(1-methyl-1H-indol-3-yl)ethan-1-amine **5a** (100 mg, 0.57 mmol) and benzaldehyde **2a** (67 mg, 0.63 mmol) were dissolved in EtOH (3 ml/mmol) and allowed to reflux for 12h. Then $NaBH_4$ (32.0 mg, 0.86 mmol) was added at rt, and the reaction was carried out according to the general procedure to afford compound **7** (92 mg, 60% yield). ^{1}H NMR (600 MHz, DMSO-d_6) δ 9.13 (bs, 1H), 7.57-7.54 (m, 3H), 7.45-7.40 (m, 4H), 7.21 (s, 1H), 7.17 (t, 1H, *J* = 7.5 Hz), 7.05 (t, 1H, *J* = 7.5 Hz), 4.20 (s, 2H), 3.74 (s, 3H), 3.15 (t, 2H, *J* = 7.5 Hz), 3.08 (t, 2H, *J* = 7.2 Hz); ^{13}C NMR (150 MHz, DMSO-d_6) δ 136.7, 132.3, 130.0 (2C), 129.0, 128.7 (2C), 127.7, 127.0, 121.4, 118.6, 118.4, 109.8, 108.6, 50.0, 47.2, 32.3, 21.6. HRMS m/z $[M+H]^+$ calcd. 265.1700, found 265.1675.

2-(1H-indol-3-yl)-N-(2-methoxybenzyl)ethan-1-amine hydrochloride (8). 2-(1H-indol-3-yl)ethan-1-amine **1a** (50 mg, 0.31 mmol) and 2-methoxy benzaldehyde **2b** (52 mg, 0.3 mmol) were dissolved in MeOH (3 ml/mmol) and the mixture was stirred at rt for 12h. $NaBH_4$ (20 mg, 0.53 mmol) was then added, and the reaction was carried out according to the general

View Article Online
DOI: 10.1039/D5MD00797F

procedure to afford compound **8** (77 mg, 78% yield). ^{1}H NMR (400 MHz, DMSO-d_6) δ 11.0 (s, 1H), 9.20 (bs, 2H), 7.56 (d, 1H, *J* = 7.6 Hz), 7.51 (d, 1H, *J* = 7.6 Hz), 7.44-7.40 (m, 1H), 7.38-7.36 (m, 1H), 7.23 (d, 1H, *J* = 2.0 Hz), 7.11-7.07 (m, 2H), 7.02-6.98 (m, 2H), 4.18-4.14 (m, 2H), 3.82 (s, 3H), 3.15-3.13 (m, 4H); ^{13}C NMR (100 MHz, DMSO-d_6) δ 157.5, 136.3, 131.5, 130.8, 126.7, 123.3, 121.2, 120.4, 119.8, 118.5, 118.2, 111.6, 111.1, 109.3, 55.6, 47.0, 44.9, 21.5 HRMS m/z $[M+H]^+$ calcd. 281.1649, found 281.1669.

N-(2-methoxybenzyl)-2-(1-methyl-1H-indol-3-yl)ethan-1-amine hydrochloride (9). 2-(1-methyl-1H-indol-3-yl)ethan-1-amine **5b** (343 mg, 1.96 mmol) and 2-methoxy-benzaldehyde **2b** (295 mg, 2.16 mmol) were dissolved in EtOH (3 ml/mmol) and allowed to reflux for 12h. $NaBH_4$ (112 mg, 2.95 mmol) was then added at rt, and the reaction was carried out according to the general procedure to afford compound **9** (302 mg, 47% yield). ^{1}H NMR (400 MHz, DMSO-d_6) δ 9.25 (bs, 2H), 7.58 (d, 1H, *J* = 7.6 Hz), 7.53-7.50 (m, 1H), 7.44-7.40 (m, 2H), 7.21 (s, 1H), 7.18-7.14 (m, 1H), 7.09-6.98 (m, 3H), 4.17-4.14 (m, 2H), 3.82 (s, 3H), 3.74 (s, 3H), 3.17-3.09 (m, 4H). ^{13}C NMR (100 MHz, DMSO-d_6) δ 157.5, 136.7, 131.5 130.7, 127.6, 127.0, 121.3, 120.4, 119.8, 118.6, 118.4, 111.1, 109.8, 108.7, 55.6, 46.9, 44.8, 32.3, 21.3. HRMS m/z $[M+H]^+$ calcd. 295.1766, found 295.1762.

2-(1H-indol-3-yl)-N-(4-nitrobenzyl)ethan-1-amine hydrochloride (10). 2-(1H-indol-3-yl)ethan-1-amine **1a** (50 mg, 0.31 mmol) and 4-nitrobenzaldehyde **2c** (47 mg, 0.31 mmol) were dissolved in MeOH (3 ml/mmol) and the mixture was stirred at rt for 12h. $NaBH_4$ (20 mg, 0.53 mmol) was then added, and the reaction was carried out according to the general procedure to afford compound **10** (82 mg, 80% yield). ^{1}H NMR (400 MHz, DMSO-d_6) δ 11.0 (s, 1H), 9.53 (bs, 2H), 8.31 (d, 2H, *J* = 8.8 Hz), 7.86 (d, 2H, *J* = 8.8 Hz), 7.58 (d, 1H, *J* = 8.0 Hz), 7.37 (d, 1H, *J* = 8.0 Hz), 7.24 (d, 1H, *J* = 2.0 Hz), 7.10 (t, 1H, *J* = 7.4 Hz), 7.01 (t, 1H, *J* = 7.8 Hz), 4.36 (s, 2H), 3.23-3.18 (m, 2H), 3.15-3.11 (m, 2H); ^{13}C NMR (100 MHz, DMSO-d_6) δ 147.7, 139.7, 136.4, 131.3 (2C), 126.7, 123.6 (2C), 123.4, 121.2, 118.5, 118.1, 111.6, 109.2, 48.9, 47.2, 21.5. HRMS m/z $[M+H]^+$ calcd. 296.1394, found 296.1379.

2-(1-methyl-1H-indol-3-yl)-N-(4-nitrobenzyl)ethan-1-amine hydrochloride (11). 2-(1-methyl-1H-indol-3-yl)ethan-1-amine **5a** (100 mg, 0.57 mmol) and 4-nitrobenzaldehyde **2c** (95 mg, 0.53 mmol) were dissolved in EtOH (3 ml/mmol) and the mixture was stirred at rt for 12 h. $NaBH_4$ (54 mg, 0.86 mmol) was then added, and the reaction was carried out according to the general procedure to afford compound **11** (30 mg, 17% yield). ^{1}H NMR (600 MHz, DMSO-d_6) δ 9.33 (bs, 2H), 8.32 (d, 2H, *J* = 8.4 Hz), 7.84 (d, 2H, *J* = 8.4 Hz), 7.59 (d, 1H, *J* = 7.6 Hz), 7.42 (d, 1H, *J* = 8.4 Hz), 7.23 (s, 1H), 7.18 (t, 1H, *J* = 7.4 Hz), 7.06 (t, 1H, *J* = 7.6 Hz), 4.37 (s, 2H), 3.75 (s, 3H), 3.24-3.05 (m, 4H); ^{13}C NMR (150 MHz, DMSO-d_6) δ 147.7, 139.6, 136.7, 131.3 (2C), 127.7, 127.0, 123.6 (2C), 121.4, 118.6, 118.4, 109.8, 108.6, 48.9, 47.2, 32.3, 21.5. HRMS m/z $[M+H]^+$ calcd. 310.1551, found 310.1546.

N-(4-chlorobenzyl)-2-(1H-indol-3-yl)ethan-1-amine hydrochloride (12). 2-(1H-indol-3-yl)ethan-1-amine **1a** (120 mg, 0.74 mmol) and 4-chlorobenzaldehyde **2d** (119 mg, 0.84 mmol) were dissolved in EtOH (3 ml/mmol) and allowed to reflux for 12h. $NaBH_4$ (42 mg, 1.12 mmol) was then added, and the reaction was carried out according to the general procedure to afford compound **12** (142 mg, 62% yield). ^{1}H NMR (400 MHz, DMSO-d_6) δ 11.0 (s, 1H), 9.17 (bs, 2H), 7.59-7.50 (m, 4H), 7.36 (d, 1H, *J* = 8.0 Hz), 7.21 (d, 1H, *J* = 1.8 Hz), 7.13-7.07 (m, 1H), 7.04-6.98

View Article Online
DOI: 10.1039/D5MD00797F

(m, 1H), 4.19 (s, 2H), 3.16-3.13 (m, 2H), 3.10-3.08 (m 2H); ^{13}C NMR (100 MHz, DMSO-d_6) δ 136.3, 133.7, 132.0 (2C), 131.3, 128.7 (2C), 126.7, 123.3, 121.2, 118.5, 118.1, 111.6, 109.3, 49.1, 47.0, 21.8. HRMS m/z $[M+H]^+$ calcd. 285.1154, found 285.1135

N-(4-chlorobenzyl)-2-(1-methyl-1H-indol-3-yl)ethan-1-amine hydrochloride (13). 2-(1-methyl-1H-indol-3-yl)ethan-1-amine **5a** (100 mg, 0.57 mmol) and 4-chlorobenzaldehyde **2d** (89 mg, 0.63 mmol) were dissolved in EtOH (3 ml/mmol) and the mixture was stirred at rt for 12 h. $NaBH_4$ (32 mg, 0.86 mmol) was then added, and the reaction was carried out according to the general procedure to afford compound **13** (37 mg, 20% yield). ^{1}H NMR (600 MHz, DMSO-d_6) δ 9.61 (bs, 2H), 7.63 (d, 2H, *J* = 8.4 Hz), 7.60 (d, 1H, *J* = 7.8 Hz), 7.51 (d, 2H, *J* = 8.4 Hz), 7.41 (d, 1H, *J* = 8.4 Hz), 7.20 (s, 1H), 7.17 (t, 1H, *J* = 7.5 Hz), 7.04 (t, 1H, *J* = 6.6 Hz), 4.18 (s, 2H), 3.74 (s, 3H), 3.15-3.09 (m, 4H); ^{13}C NMR (150 MHz, DMSO-d_6) δ 136.7, 133.6, 132.1 (2C), 131.2, 128.6 (2C), 127.6, 127.1, 121.3, 118.6, 118.4, 109.8, 108.7, 49.0, 46.9, 32.3, 21.5. HRMS m/z $[M+H]^+$ calcd. 299.1310, found 299.1300.

2-(1-methyl-1H-indol-3-yl)-N-(4-methylbenzyl)ethan-1-amine hydrochloride (14). 2-(1-methyl-1H-indol-3-yl)ethan-1-amine **5a** (70 mg, 0.40 mmol) and 4-methylbenzaldehyde **2e** (53 mg, 0.44 mmol) were dissolved in EtOH (3 ml/mmol) and the mixture was stirred at rt for 12 h. $NaBH_4$ (23 mg, 0.60 mmol) was then added, and the reaction was carried out according to the general procedure to afford compound **14** (23 mg, 23% yield). ^{1}H NMR (600 MHz, DMSO-d_6) δ 9.10 (bs, 2H), 7.56 (d, 1H, *J* = 7.8 Hz), 7.43-7.40 (m, 3H), 7.25 (d, 2H, *J* = 7.7 Hz), 7.20 (s, 1H), 7.18-7.15 (m, 1H), 7.06-7.03 (m, 1H), 4.13 (s, 2H), 3.74 (s, 3H), 3.11-3.08 (m, 4H), 2.32 (s, 3H); ^{13}C NMR (150 MHz, DMSO-d_6) δ138.3, 136.7, 129.9 (2C), 129.2 (3C), 127.6, 127.0, 121.4, 118.6, 118.4, 109.8, 108.7, 49.7, 46.9, 32.3, 21.6, 20.8. HRMS m/z $[M+H]^+$ calcd. 279.1856, found 279.1838.

N-(3-chloro-4,5-dimethoxybenzyl)-2-(1H-indol-3-yl)ethan-1-amine hydrochloride (15). 2-(1H-indol-3-yl)ethan-1-amine **1a** (200 mg, 1.25 mmol) and 3-chloro-4,5-dimethoxybenzaldehyde **2f** (250 mg, 1.25 mmol) were dissolved in MeOH (3 ml/mmol) and the mixture was stirred at rt for 48h. $NaBH_4$ (81 mg, 2.13 mmol) was then added, and the reaction was carried out according to the general procedure to afford compound **15** (97 mg, 77% yield). ^{1}H NMR (400 MHz, DMSO-d_6) δ 11.0 (s, 1H), 9.64, (bs, 2H), 7.58 (d, 1H, *J* = 7.6 Hz), 7.47 (d, 1H, *J* = 1.4 Hz), 7.37 (d, 1H, *J* = 8.4 Hz), 7.29-7.24 (m, 2H), 7.10 (t, 1H, *J* = 7.6 Hz), 7.00 (t, 1H, *J* = 7.6 Hz), 4.14 (s, 2H), 3.87 (s, 3H), 3.76 (s, 3H), 3.22-3.05 (m, 4H); ^{13}C NMR (100 MHz, DMSO-d_6) δ 153.4, 144.9, 136.3, 129.0, 126.7 (2C), 123.3, 123.0, 121.2, 118.4, 118.2, 114.0, 111.6, 109.3, 60.3, 56.3, 49.1, 46.8, 21.6. HRMS m/z $[M+H]^+$ calcd. 345.1365, found 345.1363.

N-(3-chloro-4,5-dimethoxybenzyl)-2-(1-methyl-1H-indol-3-yl)ethan-1-amine hydrochloride (16). 2-(1-methyl-1H-indol-3-yl)ethan-1-amine **5a** (200 mg, 1.14 mmol) and 3-chloro-4,5-dimethoxybenzyl) **2f** (253 mg, 1.26 mmol) were dissolved in EtOH (3 ml/mmol) and the mixture was stirred at rt for 12h. $NaBH_4$ (23 mg, 0.60 mmol) was then added, and the reaction was carried out according to the general procedure to afford compound **16** (140 mg, 34% yield). ^{1}H NMR (600 MHz, DMSO-d_6) δ 9.21 (bs, 2H), 7.57 (d, 1H, *J* = 7.8 Hz), 7.42 (d, 1H, *J* = 7.8 Hz), 7.37-7.33 (m, 1H), 7.25 (s, 1H), 7.23 (s, 1H), 7.16 (t, 1H, *J* = 7.8 Hz), 7.06 (t, 1H, *J* = 7.2 Hz), 4.14 (s, 2H), 3.86 (s, 3H), 3.76 (s, 3H), 3.75 (s, 3H), 3.15-3.13 (m, 2H), 3.11-3.10 (m, 2H); ^{13}C NMR (150 MHz, DMSO-d_6) δ 153.4, 144.9, 136.7, 129.0, 127.7, 127.0, 126.7, 123.0, 121.3,

View Article Online
DOI: 10.1039/D5MD00797F

118.6, 118.4, 114.0, 109.8, 108.7, 60.2, 56.3, 49.1, 46.8, 32.3, 21.4. HRMS m/z $[M+H]^+$ calcd. 359.1521, found 359.1538.

2-(1-methyl-1H-indol-3-yl)-N-(naphthalen-2-ylmethyl)ethan-1-amine hydrochloride (17). 2-(1-methyl-1H-indol-3-yl)ethan-1-amine **5a** (100 mg, 0.57 mmol) and 2-naphthaldehyde **2g** (117 mg, 0.74 mmol) were dissolved in EtOH (3 ml/mmol) and allowed to reflux for 12h. $NaBH_4$ (33 mg, 0.86 mmol) was then added, and the reaction was carried out according to the general procedure to afford compound **17** (47 mg, 23% yield). ^{1}H NMR (400 MHz, DMSO-d_6) δ 9.18 (bs, 2H), 8.07 (s, 1H), 8.01 (d, 1H, *J* = 8.8 Hz), 7.98-7.92 (m, 2H), 7.70-7.66 (m, 1H), 7.61-7.55 (m, 3H), 7.42 (d, 1H, *J* = 8.4 Hz), 7.21 (s, 1H), 7.17 (t, 1H, *J* = 7.6 Hz), 7.06-7.00 (m, 1H), 4.38 (s, 2H), 3.74 (s, 3H), 3.22 (t, 2H, *J* = 7.6 Hz), 3.11 (t, 2H, *J* = 7.6 Hz); ^{13}C NMR (150 MHz, DMSO-d_6) δ 136.7, 132.8, 132.6, 129.7, 129.4, 128.4, 127.8, 127.7 (2C), 127.2, 127.0, 126.8, 126.7, 121.4, 118.6, 118.3, 109.8, 108.6, 50.1, 47.0, 32.3, 21.6. HRMS m/z $[M+]^+$ calcd. 315.1259, found 315.1236.

General procedure for synthesis of indoles 18-26

The corresponding substituted indole hydrochloride (1.0 eq) and 2-methoxybenzaldehyde (1.3 eq) were dissolved in MeOH (2 ml/mmol), along with TEA (1.1 eq). The reaction mixture was stirred at rt for 3 h, followed by the addition of $NaBH_4$ (1.5 eq), and stirring was continued for an additional 1 h at rt. After completion, the reaction was quenched with a saturated solution of $NaHCO_3$ and EtOAc was added. The water phase was extracted three times with EtOAc (3×150 ml), and the combined organic layers washed once with brine, dried over Na_2SO_4, filtered, and concentrated. The yellow residue was dissolved in EtOAc (1 ml) and treated with 2M HCl (1.0 eq) in diethyl ether at 0°C, then sonicated, filtered, and finally recrystallized from IPA to give the desired compounds.

2-(5-chloro-1H-indol-3-yl)-N-(2-methoxybenzyl)ethan-1-amine hydrochloride (18). 2-(5-chloro-1H-indol-3-yl)ethan-1-amine hydrochloride **1c** (120 mg, 0.61 mmol) and 2-methoxybenzaldehyde **2b** (0. 11 g, 0.87 mmol) were dissolved in MeOH (2 ml/mmol), along with TEA (104 µL, 0.74 mmol). The reaction was stirred at rt for 3h, after which $NaBH_4$ (35 mg, 0.92 mmol) was added, and the reaction was carried out according to the general procedure to afford compound **18** (130 mg, 60% yield). ^{1}H NMR (400 MHz, DMSO-d_6) δ 11.2 (s, 1H), 8.9 (s, 1H), 7.63 (s, 1H), 7.48-7.38 (m, 3H), 7.33 (s, 1H), 7.10 (d, 2H, *J* = 8.4 Hz), 7.02 (t, 1H, *J* = 7.4 Hz), 4.18 (s, 2H), 3.84 (s, 3H), 3.17-3.13 (m, 2H), 3.10-3.06 (m, 2H); ^{13}C NMR (150 MHz, DMSO-d_6) δ 157.5, 134.8, 131.4, 130.8, 127.9, 125.4, 123.3, 121.2, 120.4, 120.0, 117.5, 113.1, 111.1, 109.4, 55.6, 47.0, 45.0, 21.4. HRMS m/z $[M+H]^+$ calcd. 315.1259, found 315.1236.

2-(5-chloro-1-methyl-1H-indol-3-yl)-N-(2-methoxybenzyl) ethan-1-amine hydrochloride (19).

2-(5-chloro-1-methyl-1H-indol-3-yl)ethan-1-amine **5b** (390 mg, 1.87 mmol), 2-methoxybenzaldehyde **2b** (269 µl, 2.05 mmol) and TEA (286 µl, 2.05 mmol) were dissolved in EtOH (2 ml/mmol) and allowed stir at rt for 12h. $NaBH_4$ (177 mg, 2.80 mmol) was then added, and the reaction was carried out according to the general procedure to afford compound **19** (305 mg, 45% yield). ^{1}H NMR (400 MHz, DMSO-d_6) δ 8.84 (bs, 2H), 7.65 (d, 1H, *J* = 2.0 Hz), 7.47-7.41 (m, 3H), 7.31 (s, 1H), 7.17 (dd, 1H, *J1* = 8.2, *J*2 = 2.2 Hz), 7.11 (d, 1H, *J* = 7.6 Hz), 7.04-7.00 (m, 1H), 4.18 (t, 2H, *J* = 6.0 Hz), 3.84 (s, 3H), 3.76 (s, 3H), 3.16-3.05 (m, 4H); ^{13}C NMR (150 MHz,

View Article Online
DOI: 10.1039/D5MD00797F

DMSO-d_6) δ157.5, 135.2, 131.4, 130.8, 129.6, 128.1, 123.5, 121.2, 120.4, 119.8, 117.7, 111.5, 111.1, 108.5, 55.6, 47.0, 44.9, 32.6, 21.2. HRMS m/z $[M+H]^+$ calcd. 329.1416, found 329.1420.

N-(2-methoxybenzyl)-2-(5-methyl-1H-indol-3-yl)ethan-1-amine hydrochloride (20). 2-(5-methyl-1H-indol-3-yl)ethan-1-amine hydrochloride **1c** (200 mg, 0.94 mmol), and 2-methoxybenzaldehyde **2b** (168 mg, 1.23 mmol) were dissolved in MeOH (2 ml/mmol) along with the TEA (146 µL, 1.04 mmol). The reaction was allowed to be stirred at rt for 3h, then $NaBH_4$ (54 mg, 1.42 mmol) was added, and the reaction was carried out according to the general procedure to afford compound **20** (212 mg, 67% yield). ^{1}H NMR (600 MHz, DMSO-d_6) δ 10.8 (s, 1H), 8.95 (s, 2H), 7.48 (d, 1H, *J* = 7.8 Hz), 7.43 (t, 1H, *J* = 8.1 Hz), 7.29 (s, 1H), 7.25 (d, 1H, *J* = 8.5 Hz), 7.17 (s, 1H), 7.10 (d, 1H, *J* = 8.1 Hz), 7.02 (t, 1H, *J* = 7.5 Hz), 6.92 (d, 1H, *J* = 8.4 Hz), 4.18 (s, 2H), 3.83 (s, 3H), 3.16-3.06 (m, 4H), 2.38 (s, 3H); ^{13}C NMR (150 MHz, DMSO-d_6) δ 157.5, 134.7, 131.4, 130.8, 126.9 (2C), 123.4, 122.8, 120.4, 119.8, 117.6, 111.3, 111.1, 108.7, 55.6, 47.0, 45.0, 21.5, 21.3. HRMS m/z $[M+H]^+$ calcd. 295.1805, found 295.1806.

2-(6-fluoro-1H-indol-3-yl)-N-(2-methoxybenzyl)ethan-1-amine hydrochloride (21). 2-(6-fluoro-1H-indol-3-yl)ethan-1-amine hydrochloride **1d** (200 mg, 0.93 mmol), and 2-methoxybenzaldehyde **2b** (165 mg, 1.21 mmol) were dissolved in MeOH (2 ml/mmol) along with the TEA (143 µL, 1.02 mmol). The reaction was allowed to be stirred at rt for 3h, then $NaBH_4$ (54 mg, 1.42 mmol) was added, and the reaction was carried out according to the general procedure to afford compound **21** (160 mg, 51% yield). ^{1}H NMR (400 MHz, DMSO-d_6) δ 11.1 (s, 1H), 8.91 (s, 1H), 7.54 (dd, 1H, *J* 1 = 8.8 Hz, *J* 2 = 5.6 Hz), 7.48-7.41 (m, 2H), 7.24 (d, 1H, *J* = 2.0 Hz), 7.15 (dd, 1H, *J* 1 = 10.0 Hz, *J* 2 = 2.2 Hz), 7.10 (d, 1H, *J* = 8.4 Hz), 7.01 (t, 1H, *J* = 7.2 Hz), 6.91-6.86 (m, 1H), 4.17 (s, 2H), 3.83 (s, 3H), 3.18-3.07 (m, 4H); ^{13}C NMR (100 MHz, DMSO-d_6) δ 159.0 (d, *J* 1-C-F = 236 Hz), 157.5, 136.1 (d, *J* 3-C-F = 10 Hz), 131.4, 130.8, 124.0 (d, 1C, *J* 4-C-F = 3.2 Hz), 123.6, 120.4, 119.8, 119.1 (d, *J* 3-C-F = 10 Hz), 111.1, 109.6, 107.0 (d, 1C, *J* 2-C-F = 25 Hz), 97.5 (d, *J* 2-C-F = 25 Hz), 55.6, 47.0, 45.1 21.4. HRMS m/z $[M+H]^+$ calcd. 299.1555, found 299.1551.

2-(6-fluoro-1-methyl-1H-indol-3-yl)-N-(2-methoxybenzyl) ethan-1-amine hydrochloride (22). 2-(6-fluoro-1-methyl-1H-indol-3-yl)ethan-1-amine **5d** (40 mg, 0.20 mmol), 2-methoxybenzaldehyde **2a** (35 µl, 0.27 mmol) and TEA (29 µl, 0.28 mmol) were dissolved in EtOH (2 ml/mmol) and allowed to stir at rt for 12h. Then $NaBH_4$ (12 mg, 0.31 mmol) was added, and the reaction was carried out according to the general procedure to afford compound **22** (40 mg, 55% yield). ^{1}H NMR (600 MHz, DMSO-d_6) δ 8.80 (bs, 2H), 7.55-7.44 (m, 3H), 7.31-7.30 (m, 1H), 7.22 (s, 1H), 7.11-6.89 (m, 3H), 4.16 (s, 2H), 3.82 (s, 3H), 3.72 (s, 3H), 3.13-3.08 (m, 4H); ^{13}C NMR (150 MHz, DMSO-d_6) δ 159.2 (d, *J* 1-C-F = 227 Hz), 157.5, 136.7 (d, *J* 3-C-F = 10 Hz), 131.3, 130.7, 128.2 (d, *J* 4-C-F = 3.5 Hz), 123.8, 120.4 (2C), 119.5 (d, *J* 3-*C-F* = 10 Hz), 111.1, 109.2, 107.0 (d, *J* 2-C-F = 24 Hz), 96.2 (d, *J* 2-C-F = 26 Hz), 55.6, 47.1, 45.1, 32.5, 21.5. HRMS m/z $[M+H]^+$ calcd. 313.1711, found 313.1726.

2-(5-methoxy-1H-indol-3-yl)-N-(2-methoxybenzyl)ethan-1-amine hydrochloride (23). 2-(5-methoxy-1H-indol-3-yl)ethan-1-amine **1e** (70 mg, 0.36 mmol), and 2-methoxybenzaldehyde **2a** (55 mg, 0.40 mmol) were dissolved in EtOH (2 ml/mmol) and allowed to reflux for 12h. Then, the reaction mixture was cooled down to rt and $NaBH_4$ (29 mg, 0.55 mmol) was added, and the reaction was carried out according to the general procedure to afford compound **23**

View Article Online
DOI: 10.1039/D5MD00797F

(80 mg, 70% yield). ^{1}H NMR (600 MHz, DMSO-d_6) δ 10.8 (s, 1H), 8.86 (s, 2H), 7.47 (d, 1H, *J* = 7.2 Hz), 7.43 (t, 1H, *J* = 7.8 Hz), 7.26 (d, 1H, *J* = 8.4 Hz), 7.19 (d, 1H, *J* = 1.8 Hz), 7.10 (d, 1H, *J* = 8.4 Hz), 7.04-7.00 (m, 2H), 6.75 (dd, 1H, *J* 1 = 8.7 Hz, *J* 2 = 2.1 Hz), 4.18 (s, 2H), 3.82 (s, 3H), 3.77 (s, 3H), 3.15 (t, 2H, *J* = 7.8 Hz), 3.07 (t, 2H, *J* = 7.8 Hz); ^{13}C NMR (150 MHz, DMSO-d_6) δ 157.5, 153.2, 131.4, 131.4, 130.8, 127.1, 124.0, 120.4, 119.8, 112.2, 111.3, 111.1, 108.9, 100.1, 55.6, 55.5, 47.0, 45.0, 21.6. HRMS m/z $[M+H]^+$ calcd. 311.1755, found 311.1724.

2-(5-methoxy-1-methyl-1H-indol-3-yl)-N-(2-methoxybenzyl) ethan-1-amine hydrochloride (24). 2-(5-methoxy-1-methyl-1H-indol-3-yl)ethan-1-amine **5e** (300 mg, 1.47 mmol), 2-methoxybenzaldehyde **2a** (211 µl, 1.62 mmol) and TEA (225 µl, 1.62 mmol) were dissolved in EtOH (2 ml/mmol) and allowed to stir at rt for 12h. Then $NaBH_4$ (139 mg, 2.20 mmol) was added, and the reaction was carried out according to the general procedure to afford compound **24** (80 mg, 45% yield). ^{1}H NMR (400 MHz, DMSO-d_6) δ 8.93 (bs, 2H), 7.50-7.38 (m, 2H), 7.32 (d, 1H, *J* = 9.2 Hz), 7.16 (s, 1H), 7.10-7.00 (m, 3H), 6.82 (d, 1H, *J* = 8.4 Hz), 4.18 (s, 2H), 3.82 (s, 3H), 3.78 (s, 3H), 3.71 (s, 3H), 3.12-3.02 (m, 4H); ^{13}C NMR (150 MHz, DMSO-d_6) δ 157.5, 153.3, 132.0, 131.4, 130.8, 128.2, 127.4, 120.4, 119.7, 111.3, 111.1, 110.5, 108.1, 100.5, 55.6, 55.5, 46.9, 44.9, 32.5, 21.3. HRMS m/z $[M+H]^+$ calcd. 325.1911, found 325.1912.

3-(2-((2-methoxybenzyl)amino)ethyl)-1H-indol-5-ol hydrochloride (25). 3-(2-aminoethyl)-1H-indol-5-ol hydrochloride **1f** (50 mg, 0.23 mmol) and 2-methoxy benzaldehyde **2a** (48 mg, 0.35 mmol) were dissolved in MeOH (2 ml/mmol), along with $NaCNBH_3$ (22 mg, 0.35 mmol), and the reaction mixture was stirred at rt for 30 min. After completion, the solvent was removed and water was added (20 ml). 1M HCl was added until pH 3 was reached then chloroform was used to wash the aqueous phase. The water layer was treated with a 2M NaOH solution up to pH 9 and then extracted with EtOAc, washed in turn with brine, dried over Na_2SO_4 filtered and concentrated. The crude was purified over column chromatography (eluent 90:9:1 DCM:MeOH:NH_4OH). The resulting oil, was dissolved in EtOAc (1 ml) and treated with 2M HCl in diethyl ether at 0°C, sonicated, filtered, and then recrystallized from IPA to give compound **25** (25 mg, 32% yield). ^{1}H NMR (400 MHz, DMSO-d_6) δ 10.7 (s, 1H), 8.98 (s, 2H), 8.68 (s, 1H), 7.50-7.40 (m, 2H), 7.16-7.09 (m, 3H), 7.02-7.00 (m, 1H), 6.84 (s, 1H), 6.63 (d, 1H, *J* = 8.0 Hz), 4.16 (s, 2H), 3.83 (s, 3H), 3.11-3.02 (m, 4H); ^{13}C NMR (100 MHz, DMSO-d_6) δ 157.5, 150.4, 131.4, 130.8 (2C), 127.4, 123.6, 120.4, 119.8, 111.8, 111.6, 111.1, 108.3, 102.0, 55.6, 47.0, 45.0, 21.6. HRMS m/z $[M+H]^+$ calcd. 297.1598, found 297.1594.

3-(2-((2-methoxybenzyl)amino)ethyl)-1-methyl-1H-indol-5-ol hydrochloride (26)
3-(2-aminoethyl)-1-methyl-1H-indol-5-ol **5f** (100 mg, 0.36 mmol), 2-methoxybenzaldehyde **2a** (63 µl, 0.47 mmol) and TEA (57 µl, 0.40 mmol) were dissolved in MeOH (2 ml/mmol) and was stirred at rt for 12h. $NaBH_4$ (21 mg, 0.55 mmol) was then added, and the reaction was carried out according to the general procedure to afford compound **26** (40 mg, 31% yield). ^{1}H NMR (400 MHz, DMSO-d_6) δ 8.84 (bs, 1H), 8.75 (bs, 1H), 7.46-7.41 (m, 2H), 7.20 (d, 1H, *J* = 8.4 Hz), 7.12 (s, 1H), 7.09 (s, 1H), 7.02 (t, 1H, *J* = 7.4 Hz), 6.85 (d, 1H, *J* = 2.0 Hz), 6.69 (dd, 1H, *J* 1 = 8.8 Hz, *J* 2 = 1.6 Hz), 4.17 (s, 2H), 3.84 (s, 3H), 3.68 (s, 3H), 3.12 (t, 2H, *J* = 8.0 Hz), 3.00 (t, 2H, *J* = 7.6 Hz); ^{13}C NMR (150 MHz, DMSO-d_6) δ 157.4, 150.7, 131.5, 131.4, 130.9, 127.9, 127.7, 120.4, 119.8, 111.6, 111.1, 110.2, 107.3, 102.4, 55.6, 47.0, 45.0, 38.2, 32.4, 21.4. HRMS m/z $[M+H]^+$ calcd. 311.1754, found 311.1748.

View Article Online
DOI: 10.1039/D5MD00797F

N-benzyl-N-methyl-2-(1-methyl-1H-indol-3-yl)ethan-1-amine hydrochloride (29). N-methyl-2-(1-methyl-1H-indol-3-yl)ethan-1-amine **28** (50 mg, 0.26 mmol) and benzaldehyde **2a** (35 µl, 0.34 mmol) were dissolved in EtOH (2 ml/mmol), and allowed to reflux for 12h. The reaction mixture was cooled down, and $NaBH_4$ (15 mg, 0.39 mmol) was added, and the reaction was carried out according to the general procedure to afford compound **29** (40 mg, 48% yield). ^{1}H NMR (400 MHz, DMSO-d_6) δ 10.3 (bs, 1H), 7.60-7.57 (m, 2H), 7.53 (d, 1H, *J* = 7.6 Hz), 7.48-7.46 (m, 3H), 7.40 (d, 1H, *J* = 8.4 Hz), 7.21-7.14 (m, 2H), 7.03 (t, 1H, *J* = 7.6 Hz), 4.35 (s, 2H), 3.73 (s, 3H), 3.36-3.17 (m, 4H), 2.77 (s, 3H); ^{13}C NMR (150 MHz, DMSO-d_6) δ 136.7, 131.2 (2C), 130.4, 129.5, 128.9 (2C), 127.6, 127.0, 121.5, 118.7, 118.5, 109.8, 108.4, 58.4, 54.9, 48.8, 32.4, 19.7. HRMS m/z $[M+H]^+$ calcd. 279.1856, found 279.1852.

N-benzyl-N,N-dimethyl-2-(1-methyl-1H-indol-3-yl)ethan-1-aminium (30). NaH 60% in mineral oil (34 mg, 0.83 mmol) was dissolved in dry DMF (2.5 ml/mmol). Compound N-benzyl-2-(1H-indol-3-yl)ethan-1-amine **6** (70 mg, 0.29 mmol) was also dissolved in dry DMF (0.5 ml/mmol), and at 0°C was added slowly into the solution of NaH. After completion of the addition, the mixture was stirred at rt for 30 minutes. The reaction was then cooled down to 0°C, and CH_3I (35 µl, 0.83 mmol) was added dropwise, and stirred at rt for 4 hours. After completion, the residue was dissolved in H_2O (20 ml) and extracted 3×20 ml EtOAc, the combined organic layers were washed with brine dried over Na_2SO_4, filtered, and concentrated. The obtained yellow oil was dissolved in EtOAc (1 ml), and treated with 2M HCl in diethyl ether at 0°C, sonicated, filtered, and finally recrystallized from IPA to give compound **30** (40 mg, 34% yield). ^{1}H NMR (400 MHz, DMSO-d_6) δ 7.65 (d, 1H, *J* = 8.4 Hz), 7.60-7.53 (m, 4H), 7.44 (d, 1H, *J* = 8.4 Hz), 7.26 (s, 1H), 7.19 (t, 1H, *J* = 7.6 Hz), 7.08 (t, 1H, *J* = 7.6 Hz), 4.66 (s, 2H), 3.77 (s, 3H), 3.52-3.50 (m, 2H), 3.28 (m, 2H), 3.10 (s, 6H); ^{13}C NMR (100 MHz, $CDCl_3$) δ 136.7, 133.0 (2C), 130.3, 129.0 (2C), 128.1, 127.8, 126.9, 121.5, 118.7, 118.5, 109.9, 107.6, 66.4, 63.6, 49.1, 40.1, 32.4, 18.3. HRMS m/z $[M+H]^+$ calcd. 293.2013, found 293.2017.

General procedure for the synthesis of indoles 31-33

The substituted tryptamine hydrochlorides **1c**,**d** (1.0 eq) and the corresponding benzaldehydes **2a**,**b** (1.3 eq) were dissolved in EtOH (2 ml/mmol), and allowed to reflux for 12h. After completion, the reaction was quenched with a saturated solution of $NaHCO_3$, and EtOAc (50 ml) was added. The water phase was extracted with 3×50 ml EtOAc, and the combined organic layers were washed once with brine and dried over Na_2SO_4, filtered, and concentrated. The light brown residue was dissolved in EtOAc (1 ml), and treated with 2M HCl (1.0 eq) in diethyl ether at 0°C, then sonicated, filtered, and finally recrystallized from IPA to give the desired products as racemic mixtrures.

1-(2-methoxyphenyl)-6,9-dimethyl-2,3,4,9-tetrahydro-1H-pyrido[3,4-b]indole (31). 2-(1,5-dimethyl-1H-indol-3-yl)ethan-1-amine hydrochloride **1c** (100 mg, 0.52 mmol) and 2-methoxybenzaldehyde **2b** (90 µl, 0.69 mmol) were dissolved in EtOH (2 ml/mmol), and allowed to reflux for 12h. The reaction was then carried out according to the general procedure to afford compound **31** as a racemate (110 mg, 60% yield). ^{1}H NMR (400 MHz, DMSO-d_6) δ 10.0 (bs, 1H), 8.93 (bs, 1H), 7.50 (t, 1H, *J* = 7.8 Hz), 7.38 (s, 1H), 7.34 (d, 1H, *J* = 8.4 Hz), 7.25 (d, 1H, *J* = 8.4 Hz), 7.06 (d, 1H, *J* = 8.4 Hz), 6.94 (t, 1H, *J* = 7.4 Hz), 6.66 (d, 1H, *J* = 6.4 Hz), 6.15 (s, 1H), 3.97 (s, 3H), 3.43-3.40 (m, 1H), 3.24 (s, 3H), 3.08-3.00 (m, 3H), 2.42 (s, 3H); ^{13}C NMR (100 MHz, DMSO-d_6) δ 156.9, 135.7, 131.7, 130.3, 128.3, 128.0, 125.4, 123.7, 121.2,

View Article Online
DOI: 10.1039/D5MD00797F

120.6, 118.0, 111.6, 109.4, 107.2, 56.0, 47.8, 37.8, 29.5, 21.1, 18.1. HRMS m/z $[M+H]^+$ calcd. 307.1766, found 307.1769.

7-fluoro-1-phenyl-2,3,4,9-tetrahydro-1H-pyrido[3,4-b]indole hydrochloride (32). 2-(6-fluoro-1H-indol-3-yl)ethan-1-amine hydrochloride **1d** (100 mg, 0.46 mmol) and benzaldehyde **2a** (64.2 mg, 0.60 mmol) were dissolved in EtOH (2 ml/mmol), and allowed to reflux at 90°C for 12h. The reaction was then carried out according to the general procedure to afford compound **32** as a racemate (75 mg, 53% yield). ^{1}H NMR (400 MHz, DMSO-d_6) δ 11.0 (s, 1H), 10.2 (bs, 1H), 9.43 (bs, 1H), 7.56-7.42 (m, 6H), 7.10-6.90 (m, 2H), 5.93 (s, 1H), 3.41-3.35 (m, 2H), 3.15-3.00 (m, 2H); ^{13}C NMR (100 MHz, DMSO-d_6) δ 159.3 (d, *J* 1-C-F = 240 Hz), 136.5 (d, *J* 3-C-F = 10 Hz), 134.5, 130.0 (2C), 129.8 (2C), 129.0 (d, *J* 4-C-F = 3.5 Hz), 119.3 (d, *J* 3-C-F = 10 Hz), 107.6 (d, *J* 2-C-F = 25 Hz), 107.4, 97.6 (d, *J* 2-C-F = 25 Hz), 79.2, 55.4, 18.0. HRMS m/z $[M+H]^+$ calcd. 267.1293, found 267.1019.

7-fluoro-1-(2-methoxyphenyl)-2,3,4,9-tetrahydro-1H-pyrido[3,4-b]indole (33). 2-(6-fluoro-1H-indol-3-yl)ethan-1-amine hydrochloride **1d** (100 mg, 0.46 mmol) and 2-methoxybenzaldehyde **2b** (115 mg, 0.84 mmol) were dissolved in EtOH (2 ml/mmol), and allowed to reflux for 12h. The reaction was then carried out according to the general procedure to afford compound **33** as a racemate (85 mg, 55% yield). ^{1}H NMR (400 MHz, DMSO-d_6) δ 11.0 (s, 1H), 10.0 (bs, 1H), 9.0 (bs, 1H), 7.56-7.45 (m, 2H), 7.21 (d, 1H, *J* = 8.3 Hz), 7.08 (dd, 1H, *J* 1 = 10.0 Hz, *J* 2 = 2.4 Hz), 6.97 (t, 1H, *J* = 7.5 Hz), 6.94-6.88 (m, 2H), 6.03 (s, 1H), 3.92 (s, 3H), 3.49-3.38 (m, 1H), 3.28-3.17 (m, 1H), 3.12-2.95 (m, 2H); ^{13}C NMR (100 MHz, DMSO-d_6) δ 159.4 (d, *J* 1-C-F = 242 Hz), 157.2 (2C), 136.4 (d, *J* 3-C-F = 10 Hz), 131.4, 130.4, 128.6, 122.5, 120.5, 119,3 (d, *J* 3-C-F = 10 Hz), 111.5 (2C), 107.9, 107.4 (d, *J* 2-C-F = 25 Hz), 97.6 (d, *J* 2-C-F = 25 Hz), 56.0 (2C), 49.2, 18.2. HRMS m/z $[M+H]^+$ calcd. 297.1398, found 297.1388.

In Silico Predictions and Cell Viability Assay

In silico predictions of toxicity endpoints for selected indole-based inhibitors were performed using ProTox 3.0 (https://tox.charite.de/protox3/),[35] which estimates various toxicity classes based on molecular structure. SwissADME (https://www.swissadme.ch/)[36] was used to evaluate physicochemical properties and lead-likeness.

Cell viability was assessed using the resazurin reduction assay in *Spodoptera frugiperda* (Sf9) and human embryonic kidney (HEK293) cells. Both cell types were seeded at 20 000 cells per well in 96-well plates and allowed to attach and reach approximately 50% confluence before compound addition. Cells were treated with three concentrations of inhibitor **15** for 24 h. Cells receiving the same DMSO concentration as experimental wells but no inhibitor served as vehicle controls (100% viability reference). Staurosporine (STS) was included as a positive cytotoxic control, and propranolol (Prop) as a non-cytotoxic reference treatment. Sf9 cells were maintained at 27 °C, and HEK293 cells at 37 °C, in their respective culture media. After compound exposure, resazurin solution was added directly to each well to a final concentration of 40 µM (10 µg/mL), and plates were incubated for 3 h under standard culture conditions. Fluorescence was measured at an excitation wavelength of 535 nm and an emission wavelength of 595 nm using a microplate reader. Cell viability was expressed as a percentage relative to DMSO vehicle controls. All substances were analyzed in triplicate on two separate occasions (three wells per concentration per experiment).

View Article Online
DOI: 10.1039/D5MD00797F

Protein expression

The expression of the recombinant AChE1 enzyme from mosquitoes (*An. gambiae, and Ae. aegypti*), and the recombinant vertebrate enzyme *h*AChE was performed as described in the previous publication.[37]

IC_{50} determination

The in vitro biochemical evaluation has been performed using activity-based Ellman assay.[38] The IC_{50} values for the synthesized indoles derivatives were determined on the recombinant *Ag*AChE1, *Aa*AChE1 and *h*AChE according to the following procedure. Freshly prepared stock solutions of the indole compounds were prepared from solid material dissolved in DMSO at a concentration of 100 mM. The dilutions series were prepared in 0.1 M sodium phosphate buffer (pH 7.4). The eight different concentrations of indole compounds were used with maximum of 1 mM. The activity measurements were performed using the non-purified recombinant enzyme in growth medium, and the enzymatic activity was measured using the Ellman assay, readjusted to a 96-wells format. The compounds were incubated along with the enzyme for 5 min at rt, then the reaction was initiated with the addition of acetylcholine iodide (ATChI) as the substrate and the enzymatic reaction was measured by monitoring changes in the absorbance of individual wells at 412 nm over 65 s in the same synergy H4 plate reader (Molecular Devices). The assay was performed at 30°C in a final assay volume of 200 µl of 0.1 M phosphate buffer (pH 7.4) containing 0.2 mM of the reagent 5,5'-dithiobis (2-nitrobenzoic acid) and 1 mM of the substrate acetylthiocholine iodide. The average slope determined for eight positive controls (where, inhibitor was replaced with phosphate buffer) on each plate was taken to represent 100% activity and the activity observed in the sample wells were quantified in relation to this value. IC_{50} values were calculated using nonlinear regression (curve-fitting) in GraphPad prism and the log [inhibitor] vs. response variable slop equation was fitted using four parameters.

Generation, collection, and refinement of crystal structures.

The catalytic domain of AChE from *m*AChE was expressed in HEK293F cells, purified, and crystallized following previously established protocols.[39] Briefly, HEK293F cells were cultured in suspension using Freestyle 293 and Glutamax media (Gibco), supplemented with 20 µg/ml Gentamicin (Gibco). The *m*AChE-containing culture supernatant was harvested by centrifugation, and the enzyme was purified from the clarified supernatant through a series of affinity and size-exclusion chromatography steps. Protein crystallization was performed using the hanging drop vapor diffusion method. The protein solution, at a concentration of 10 mg/ml, was mixed with a reservoir solution composed of 27–30% (w/v) PEG750MME and 0.1 M HEPES buffer, pH 6.9-7.1. To form binary (inhibitor·AChE) complexes, inhibitors were soaked into the pre-formed *m*AChE crystals prior to flash freezing in liquid nitrogen, as described in earlier studies.[40] X-ray diffraction data were collected at the MAXIV synchrotron (Lund, Sweden) using the Biomax beamline equipped with an Eiger detector. The collected data were indexed and integrated using XDS[41] and scaled with aimless.[42] Initial phases were determined by rigid-body refinement using a modified apo structure of *m*AChE (PDB: 1J06) as a starting model. Further crystallographic refinement and manual model building were conducted using the Phenix software[43] suite and COOT.[44] Model validation was performed

View Article Online
DOI: 10.1039/D5MD00797F

with MolProbity (integrated within Phenix) and the wwPDB Validation Service (https://validate-rcsb-1.wwpdb.org/).

Molecular dynamics (MD) simulations

System preparation for MD simulations. MD simulations of *m*AChE•**9** were based on coordinates from the X-ray structure (PDB: 9SNJ). Coordinates for *Ag*AChE1•**9** was obtained by superposing the X-ray structure of apo *Ag*AChE1 (PDB: 5YDI) against *m*AChE•**9**. The binding pose of inhibitor **9** was thereafter merged with *Ag*AChE1, followed by altering the conformation of $Tyr489_{Ag}$ (corresponding to $Tyr337_{m}$) to avoid clashes. Inhibitor **9** was geometry optimized followed by calculation of electrostatic surface potentials (ESPs) using the HF/6-31G* basis set with Gaussian 09. The secondary amine in the linker of **9** was protonated, i.e. positively charged. Partial atomic charges were calculated using the restrained electrostatic potential (RESP) method using the antechamber program of AmberTools. Other parameters were assigned by the General Amber Force Field (GAFF). Files were converted to GROMACS format using the acpype python script. Pdb2gmx within GROMACS was used for generation of topology and coordinate files, with the AMBER99SB-ILDN force field.[45]

MD simulations. Each system was solvated using a dodecahedral periodic box of TIP3P water. Sodium ions were added to neutralize the system that were then energy minimized using the steepest decent algorithm. Heating to 300 K was thereafter performed over a 100 ps NVT simulation. This was followed by a 500 ps NPT simulation to equilibrate the pressure to 1 atm. During both of these simulations the heavy atoms were restrained at their starting positions with a force constant of 1000 kJ mol^{-1} nm^2. These restraints were stepwise removed over a 1 ns NPT simulation. The Berendsen thermostat was used for regulating temperature and pressure. A time step of 2 fs was used for all simulations, constraining bonds using the parallel LINCS algorithm. Short range non-bonded interactions were computed for atom pairs within a cutoff of 14 Å. Long-range electrostatic interactions were calculated using the Particle-Mesh-Ewald summation method, using fourth-order cubic interpolation with a 1.2 Å grid spacing. Five replicates of 100 ns MD simulations were performed for *m*AChE•**9** and *Ag*AChE1•**9**, respectively, with varying initial velocities. All simulations were run with GROMACS 5.1.4.[45]

Analysis. Root-mean-square deviation (RMSD) values were calculated using the gmx rms module in GROMACS,[45] superposing against the main chain atoms of the NPT equilibrated structure. According to the resulting RMSD values the simulation converged after 50 ns. Thus, all subsequent analyses were performed using the concatenated 50-100 ns of each simulation. Root-mean-square fluctuation (RMSF) values were calculated using the gmx rmsf module. Pairwise minimum distances between selected atoms were calculated using the gmx pairdist module. Principal component analysis (PCA) was performed by calculating the mass-weighted covariance matrix of heavy atoms of inhibitor **9** using the gmx covar module, after superposing the trajectory against the main chain heavy atoms of the NPT equilibrated structure. Eigenvectors and eigenvalues were generated, and projections of the trajectory to eigenvector 1-3 were calculated using the gmx anaeig module. Cluster analysis of the generated binding poses of **9** was performed using gmx_clusterByFeatures[46] including eigenvector 1-3, using the K-means algorithm and the Elbow method with a threshold of 3.0 % on the sum of square residual to sum of square total ratio. The water occupancy was calculated using the gmx trjorder module, using a cutoff of 3.5 Å as the specified hydrogen bonding distance for selected heavy atoms.

View Article Online
DOI: 10.1039/D5MD00797F

In vivo experiments

Ae. aegypti Mombasa strain and *An. gambiae* Kisumu strain from Kenya were used to test the insecticidal activities of the compounds. These mosquitoes have been colonized at KEMRI for over 20 years and are routinely tested to verify their susceptibility to permethrin and deltamethrin in accordance with WHO tube bioassay guidelines using diagnostic concentrations of 0.75% permethrin and 0.05% deltamethrin impregnated on filter paper. Mosquito rearing was carried out in an insectary maintained at 27-28 °C ca. 80% humidity, on a 12/12 h light/darkness cycle, and maintained at optimal larval concentrations to avoid possible effects of competition. For mosquito tests, nonblood fed, five-day old female mosquitoes were used, and testing was performed in batches of approximately five mosquitoes (100 in total per compound). Five mosquitoes were placed in a 500 ml paper cup and anesthetized by placing the cup in a -20 °C freezer for 3 min. Thereafter, for the topical application tests, the mosquitoes were gently poured onto a plate refrigerated at -20 °C overlaid with a paper towel, and the compound solution (acetone, 0.1 µl) was deposited on the upper part of the pronotum using a micro-pipette. As a negative control, 0.1 µl of pure acetone was applied on some mosquitoes, and as a positive control propoxur insecticide was used (Tables S9-S10). After the topical application, the mosquitoes were returned to the paper cups and placed back in the insectary, where they were given with a glucose meal and maintained under standard conditions. Mosquito mortality was recorded after 24 h.

Supporting information

The supporting material contains chemical structures of starting materials; supplementary schemes of synthesis; dose-response IC_{50} curves for inhibition kinetics; table of data collection and refinement statistics of X-ray crystallography structures; MD simulations data; in vivo raw data tables; NMR spectra.

Conflict of interest

There is no conflict of interest to declare.

Acknowledgments

The authors are grateful to Dr. Tomas Kindahl for synthetic contribution in the start of the project, and to Dr. Annica Rönnbäck for conducting the cell viability experiments. This work was funded by grants from the Swedish Research Council (2017-00664). We acknowledge MAX IV Laboratory for time on the BioMAXBeam line. Research conducted at MAX IV, a Swedish national user facility, is supported by the Swedish Research council under contract 2018-07152, the Swedish Governmental Agency for Innovation Systems under contract 2018-04969 and Formas under contract 2019-02496. The research was also enabled by resources provided by the Swedish National Infrastructure for Computing (SNIC), partially funded by the Swedish Research Council via grant agreement no. 2018-05973. Computations were conducted using the resources of the High Performance Computing Center North (HPC2N).

References

(1) S. Bhatt, D. J. Weiss, E. Cameron, D. Bisanzio, B. Mappin, U. Dalrymple, K. E. Battle, C. L. Moyes, A. Henry, P. A. Eckhoff, E. A. Wenger, O. Briët, M. A. Penny, T. A. Smith, A. Bennett, J. Yukich, T. P. Eisele, J. T. Griffin, C. A. Fergus, M. Lynch, F. Lindgren, J. M. Cohen, C. L. J. Murray, D. L. Smith, S. I. Hay, R. E. Cibulskis, P. W. Gething. The effect of malaria control on *Plasmodium falciparum* in Africa between 2000 and 2015. *Nature* 2015, **526** (7572), 207-211.
(2) A. S. Ssemata, A. J. Nakitende, S. Kizito, M. R. Thomas, S. Islam, P. Bangirana, N. Nakasujja, Z. Yang, Y. Yu, T. M. Tran. Association of severe malaria with cognitive and behavioural outcomes in low-and middle-income countries: a meta-analysis and systematic review. *Malaria Journal* 2023, **22** (1), 227.
(3) S. Mrema, F. Okumu, J. Schellenberg, G. Fink. Associations between the use of insecticide-treated nets in early childhood and educational outcomes, marriage and child-bearing in early adulthood: evidence from a 22-year prospective cohort study in Tanzania. *Malaria Journal* 2023, **22** (1), 134.
(4) M. Weill, G. Lutfalla, K. Mogensen, F. Chandre, A. Berthomieu, C. Berticat, N. Pasteur, A. Philips, P. Fort, M. Raymond. Comparative genomics: Insecticide resistance in mosquito vectors. *Nature* 2003, **423** (6936), 136-137.
(5) W. C. Black IV, T. K. Snell, K. Saavedra-Rodriguez, R. C. Kading, C. L. Campbell. From global to local—new insights into features of pyrethroid detoxification in vector mosquitoes. *Insects* 2021, **12** (4), 276.
(6) T. R. Fukuto. Mechanism of action of organophosphorus and carbamate insecticides. *Environ. Health Perspect.* 1990, **87**, 245-254.
(7) D. Dou, J. G. Park, S. Rana, B. J. Madden, H. Jiang, Y.-P. Pang. Novel selective and irreversible mosquito acetylcholinesterase inhibitors for controlling malaria and other mosquito-borne diseases. *Sci. Rep.* 2013, **3**, 1068.
(8) J. E. Casida. Organophosphorus xenobiotic toxicology. *Annu. Rev. Pharmacol. Toxicol.* 2017, **57**, 309-327.
(9) H. Dvir, I. Silman, M. Harel, T. L. Rosenberry, J. L. Sussman. Acetylcholinesterase: From 3D structure to function. *Chem.-Biol. Interact.* 2010, **187** (1-3), 10-22.
(10) J. L. Sussman, M. Harel, F. Frolow, C. Oefner, A. Goldman, L. Toker, I. Silman. Atomic structure of acetylcholinesterase from *Torpedo californica*: a prototypic acetylcholine-binding protein. *Science* 1991, **253** (5022), 872-879.
(11) M. Weill, P. Fort, A. Berthomieu, M. P. Dubois, N. Pasteur, M. Raymond. A novel acetylcholinesterase gene in mosquitoes codes for the insecticide target and is non–homologous to the ace gene *Drosophila*. *Proc. R. Soc. B* 2002, **269** (1504), 2007-2016.
(12) Y. H. Kim, S. H. Lee. Which acetylcholinesterase functions as the main catalytic enzyme in the Class Insecta? *Insect Biochem. Mol. Biol.* 2013, **43** (1), 47-53.
(13) R. Kumari, C. Lindgren, R. Kumar, N. Forsgren, C. D. Andersson, F. Ekström, A. Linusson. Enzyme dynamics determine the potency and selectivity of inhibitors targeting disease-transmitting mosquitoes. *ACS Infect. Dis.* 2024, **10** (10), 3664–3680.
(14) C. Engdahl, S. Knutsson, F. Ekström, A. Linusson. Discovery of selective inhibitors targeting acetylcholinesterase 1 from disease-transmitting mosquitoes. *J. Med. Chem.* 2016, **59** (20), 9409-9421.

View Article Online
DOI: 10.1039/D5MD00797F

(15) S. Knutsson, T. Kindahl, C. Engdahl, D. Nikjoo, N. Forsgren, S. Kitur, F. Ekström, L. Kamau, A. Linusson. N -Aryl- N' -ethyleneaminothioureas effectively inhibit acetylcholinesterase 1 from disease-transmitting mosquitoes. *Eur. J. Med. Chem.* 2017, **134**, 415-427.
(16) S. Knutsson, C. Engdahl, R. Kumari, N. Forsgren, C. Lindgren, T. Kindahl, S. Kitur, L. Wachira, L. Kamau, F. Ekström, A. Linusson. Noncovalent inhibitors of mosquito acetylcholinesterase 1 with resistance-breaking potency. *J. Med. Chem.* 2018, **61** (23), 10545-10557.
(17) A. Vidal-Albalat, T. Kindahl, R. Rajeshwari, C. Lindgren, N. Forsgren, S. Kitur, L. S. Tengo, F. Ekström, L. Kamau, A. Linusson. Structure–activity relationships reveal beneficial selectivity profiles of inhibitors targeting acetylcholinesterase of disease-transmitting mosquitoes. *J. Med. Chem.* 2023, **66** (9), 6333-6353.
(18) V. Hepnarova, M. Hrabinova, L. Muckova, T. Kucera, M. Schmidt, R. Dolezal, L. Gorecki, V. Hrabcova, J. Korabecny, E. Mezeiova, D. Jun, J. Pejchal. Non-covalent acetylcholinesterase inhibitors: In vitro screening and molecular modeling for novel selective insecticides. *Toxicol. In Vitro* 2022, **85**, 105463.
(19) N. Desai, H. Somani, A. Trivedi, K. Bhatt, L. Nawale, V. M. Khedkar, P. C. Jha, D. Sarkar. Synthesis, biological evaluation and molecular docking study of some novel indole and pyridine based 1, 3, 4-oxadiazole derivatives as potential antitubercular agents. *Bioorg. Med. Chem. Lett.* 2016, **26** (7), 1776-1783.
(20) N. Rajeev, K. S. Sharath Kumar, Y. K. Bommegowda, K. S. Rangappa, M. P. Sadashiva. Catalyst free sequential one-pot reaction for the synthesis of 3-indole propanoates/propanoic acid/propanamides as antituberculosis agents. *J. Chin. Chem. Soc.* 2021, **68** (1), 39-44.
(21) R. Sakhuja, S. S. Panda, L. Khanna, S. Khurana, S. C. Jain. Design and synthesis of spiro [indole-thiazolidine] spiro [indole-pyrans] as antimicrobial agents. *Bioorg. Med. Chem. Lett.* 2011, **21** (18), 5465-5469.
(22) Y. Chen, H. Li, J. Liu, R. Zhong, H. Li, S. Fang, S. Liu, S. Lin. Synthesis and biological evaluation of indole-based peptidomimetics as antibacterial agents against Gram-positive bacteria. *Eur. J. Med. Chem.* 2021, **226**, 113813.
(23) S. Y. Nie, J. D. Zhao, X. W. Wu, Y. Yao, F. R. Wu, Y. L. Lin, X. Li, A. R. Kneubehl, M. B. Vogt, R. Rico-Hesse, Y. C. Song. Synthesis, structure-activity relationship and antiviral activity of indole-containing inhibitors of Flavivirus NS2B-NS3 protease. *Eur. J. Med. Chem.* 2021, **225**.
(24) S. Dadashpour, S. Emami. Indole in the target-based design of anticancer agents: A versatile scaffold with diverse mechanisms. *Eur. J. Med. Chem.* 2018, **150**, 9-29.
(25) C. L. Cardoso, I. Castro-Gamboa, D. H. S. Silva, M. Furlan, R. d. A. Epifanio, Â. d. C. Pinto, C. Moraes de Rezende, J. A. Lima, V. d. S. Bolzani. Indole glucoalkaloids from *Chimarrhis turbinata* and their evaluation as antioxidant agents and acetylcholinesterase inhibitors. *J. Nat. Prod.* 2004, **67** (11), 1882-1885.
(26) M. S. Islam, A. M. Al-Majid, M. Azam, V. P. Verma, A. Barakat, M. Haukka, A. A. Elgazar, A. Mira, F. A. Badria. Construction of spirooxindole analogues engrafted with indole and pyrazole scaffolds as acetylcholinesterase inhibitors. *ACS omega* 2021, **6** (47), 31539-31556.
(27) T. R. Makhanya, R. M. Gengan, K. Kasumbwe. Synthesis of fused indolo-pyrazoles and their antimicrobial and insecticidal activities against *Anopheles arabiensis* mosquito. *ChemistrySelect* 2020, **5** (9), 2756-2762.
(28) A. W. Sousa Da Silva, W. F. Vranken. ACPYPE - AnteChamber PYthon Parser interfacE. *BMC Res. Notes* 2012, **5** (1), 367.

(29) J. R. Sousa, F. A. Silva, S. K. Targanski, B. R. Fazolo, J. M. Souza, M. G. Campos, L. C. Vieira, T. A. de Oliveira Mendes, M. A. Soares. Synthesis and larvicidal activity of indole derivatives against *Aedes aegypti* (Diptera: Culicidae). *J. Appl. Entomol.* 2019, **143** (10), 1172-1181.
(30) E. Camerino, D. M. Wong, F. Tong, F. Körber, A. D. Gross, R. Islam, E. Viayna, J. M. Mutunga, J. Li, M. M. Totrov, J. R. Bloomquist, P. R. Carlier. Difluoromethyl ketones: Potent inhibitors of wild type and carbamate-insensitive G119S mutant *Anopheles gambiae* acetylcholinesterase. *Bioorg. Med. Chem. Lett.* 2015, **25** (20), 4405-4411.
(31) D. M. Wong, J. Li, Q.-H. Chen, Q. Han, J. M. Mutunga, A. Wysinski, T. D. Anderson, H. Ding, T. L. Carpenetti, A. Verma, R. Islam, S. L. Paulson, P. C. H. Lam, M. Totrov, J. R. Bloomquist, P. R. Carlier. Select small core structure carbamates exhibit high contact toxicity to “carbamate-resistant” strain malaria mosquitoes, *Anopheles gambiae* (Akron). *PLoS ONE* 2012, **7** (10), e46712.
(32) D. R. Swale, P. R. Carlier, J. A. Hartsel, M. Ma, J. R. Bloomquist. Mosquitocidal carbamates with low toxicity to agricultural pests: an advantageous property for insecticide resistance management. *Pest Manage. Sci.* 2015, **71** (8), 1158-1164.
(33) C. M. Tice. Selecting the right compounds for screening: does Lipinski's rule of 5 for pharmaceuticals apply to agrochemicals? *Pest Manage. Sci.* 2001, **57** (1), 3-16.
(34) J. A. Turner, C. N. E. Ruscoe, T. R. Perrior. Discovery to development: Insecticides for malaria vector control. *Chimia* 2016, **70** (10), 684-693.
(35) P. Banerjee, E. Kemmler, M. Dunkel, R. Preissner. ProTox 3.0: a webserver for the prediction of toxicity of chemicals. *Nucleic Acids Res.* 2024, **52** (W1), W513-W520.
(36) A. Daina, O. Michielin, V. Zoete. SwissADME: a free web tool to evaluate pharmacokinetics, drug-likeness and medicinal chemistry friendliness of small molecules. *Sci. Rep.* 2017, **7**.
(37) C. Engdahl, S. Knutsson, S.-Å. Fredriksson, A. Linusson, G. Bucht, F. Ekström. Acetylcholinesterases from the disease vectors *Aedes aegypti* and *Anopheles gambiae*: Functional characterization and comparisons with vertebrate orthologues. *PLoS ONE* 2015, **10** (10), e0138598.
(38) G. L. Ellman, K. D. Courtney, V. Andres, R. M. Featherstone. A new and rapid colorimetric determination of acetylcholinesterase activity. *Biochem. Pharmacol.* 1961, **7** (2), 88-&.
(39) F. Ekström, C. Akfur, A.-K. Tunemalm, S. Lundberg. Structural changes of phenylalanine 338 and histidine 447 revealed by the crystal structures of tabun-inhibited murine acetylcholinesterase. *Biochemistry* 2006, **45** (1), 74-81.
(40) L. Berg, C. D. Andersson, E. Artursson, A. Hörnberg, A.-K. Tunemalm, A. Linusson, F. Ekström. Targeting acetylcholinesterase: Identification of chemical leads by high throughput screening, structure determination and molecular modeling. *PLoS ONE* 2011, **6** (11), e26039.
(41) W. Kabsch. XDS. *Acta Crystallogr., Sect. D: Biol. Crystallogr.* 2010, **66** (2), 125-132.
(42) J. Agirre, M. Atanasova, H. Bagdonas, C. B. Ballard, A. Baslé, J. Beilsten-Edmands, R. J. Borges, D. G. Brown, J. J. Burgos-Mármol, J. M. Berrisford. The CCP4 suite: integrative software for macromolecular crystallography. *Acta Crystallogr., Sect. D:Struct. Biol.* 2023, **79** (6), 449-461.
(43) D. Liebschner, P. V. Afonine, M. L. Baker, G. Bunkóczi, V. B. Chen, T. I. Croll, B. Hintze, L.-W. Hung, S. Jain, A. J. McCoy. Macromolecular structure determination using X-rays,

neutrons and electrons: recent developments in Phenix. *Acta Crystallogr., Sect. D:Struct. Biol.* 2019, **75** (10), 861-877.
(44) P. Emsley, B. Lohkamp, W. G. Scott, K. Cowtan. Features and development of Coot. *Acta Crystallogr., Sect. D: Biol. Crystallogr.* 2010, **66** (4), 486-501.
(45) S. Pronk, S. Páll, R. Schulz, P. Larsson, P. Bjelkmar, R. Apostolov, M. R. Shirts, J. C. Smith, P. M. Kasson, D. Van Der Spoel, B. Hess, E. Lindahl. GROMACS 4.5: A high-throughput and highly parallel open source molecular simulation toolkit. *Bioinformatics* 2013, **29** (7), 845-854.
(46) *gmx_clusterByFeatures, https://gmx-clusterbyfeatures.readthedocs.io/en/latest/, (accessed December 2024).*

Data Availability Statement

View Article Online
DOI: 10.1039/D5MD00797F

Potent and Selective Indole-based Inhibitors Targeting Disease-Transmitting Mosquitoes

R. Rajeshwari[1], V. Duvauchelle[1], C. Lindgren[1], K. Stangner[1], S. Knutsson[1], N. Forsgren[2], F. Ekström[2], L. Kamau[3], A. Linusson*[1]

[1]*Department of Chemistry, Umeå University (Sweden);* [2]*Swedish Defense Research Agency, Umeå (Sweden);* [3]*Centre of Biotechnology Research and Development, Kenya Medical Research Institute, Nairobi, Kenya*
*Corresponding author. E-mail address: anna.linusson@umu.se

- The data supporting this article have been included as part of the Supplementary Information
- Crystallographic data for the two new protein-ligand complexes *m*AChE•**8** and *m*AChE•**9** has been deposited at the RCSB Protein Data Bank (PDB) under PDB entry codes 9SND and 9SNJ prior publication and can be obtained from https://www.rcsb.org/